Electronic Supplementary Material (ESI) for ChemComm.
This journal is © The Royal Society of Chemistry 2023

Coaxial assembly of helical aromatic foldamers by metal coordination

SUPPORTING INFORMATION

Table of contents

1. General information and instrumentation

Commercial reagents were purchased from Sigma-Aldrich, Alfa-Aesar or TCI and were used without further purification unless otherwise specified. Tetrahydrofurane (THF) and dichloromethane (CH_2Cl_2) were dried over alumina columns; chloroform ($CHCl_3$), triethylamine (Et_3N) and diisopropylethylamine (DIPEA) were distilled over calcium hydride (CaH_2) prior to use. Reactions were monitored by thin layer chromatography (TLC) on Merck silica gel 60-F254 plates and observed under UV light. Column chromatography purifications were carried out on Merck GEDURAN Si60 (40-63 μm). ESI mass spectra were obtained from the Mass Spectrometry Laboratory at the European Institute of Chemistry and Biology (UMS 3033 -IECB), Pessac, France.

2. Preparation and characterization of the complexes in solution

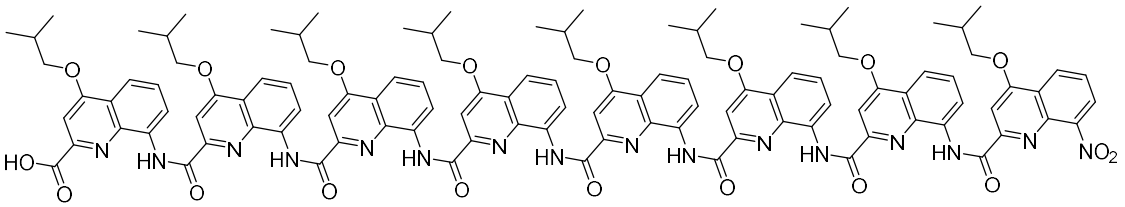

Q_8-H

Dimer complexes were prepared according one of the two following methods. The procedures are described for Q_8-H but can be adapted to any acid-functionalized oligoquinoline foldamer.

1. In an NMR tube, Q_8-H (2 mg, 1 µmol) is dissolved in 600 µL of $CDCl_3$. To this solution, a small amount of the desired salt (i.e. NaOH, 1 mg, 25 µmol) is added. The suspension is shaken for a couple of minutes. Once the complex formation occurs quantitatively as judged by NMR analysis (time varies depending on salt used), the solution can be filtered to obtain the desired dimer complex in solution without salt excess.

2. Q_8-H (2 mg, 1 µmol) is dissolved in 2 mL of dichloromethane. The solution is washed with 2 mL of an aqueous saturated solution of the metal salt, then dried over magnesium sulfate and concentrated under reduced pressure to afford the desired metal dimer complex as a solid without salt excess.

Both methods produce dimeric metal complexes quantitatively without difference in purity. The salt excess is successfully removed by using any of the two methods as proved by the addition of initial Q_8-H to the complexes resulting in a mixture of Q_8-H and dimeric complexes that are in slow exchange in the NMR time scale.

Sodium-ligated quinoline dimers:

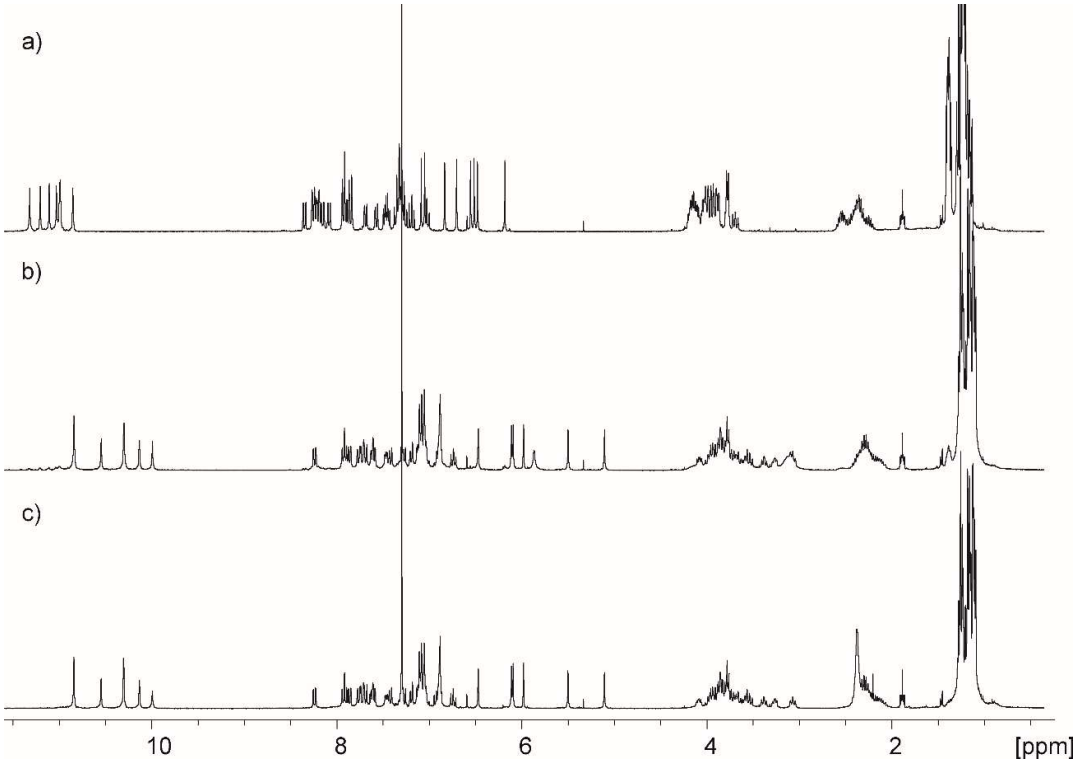

Figure S1. ^{1}H NMR spectra (300 MHz, 298K) of a $CDCl_3$ solution of a) Q_8-H b) Q_8-H and NaOH powder after 2 min c) 5 min

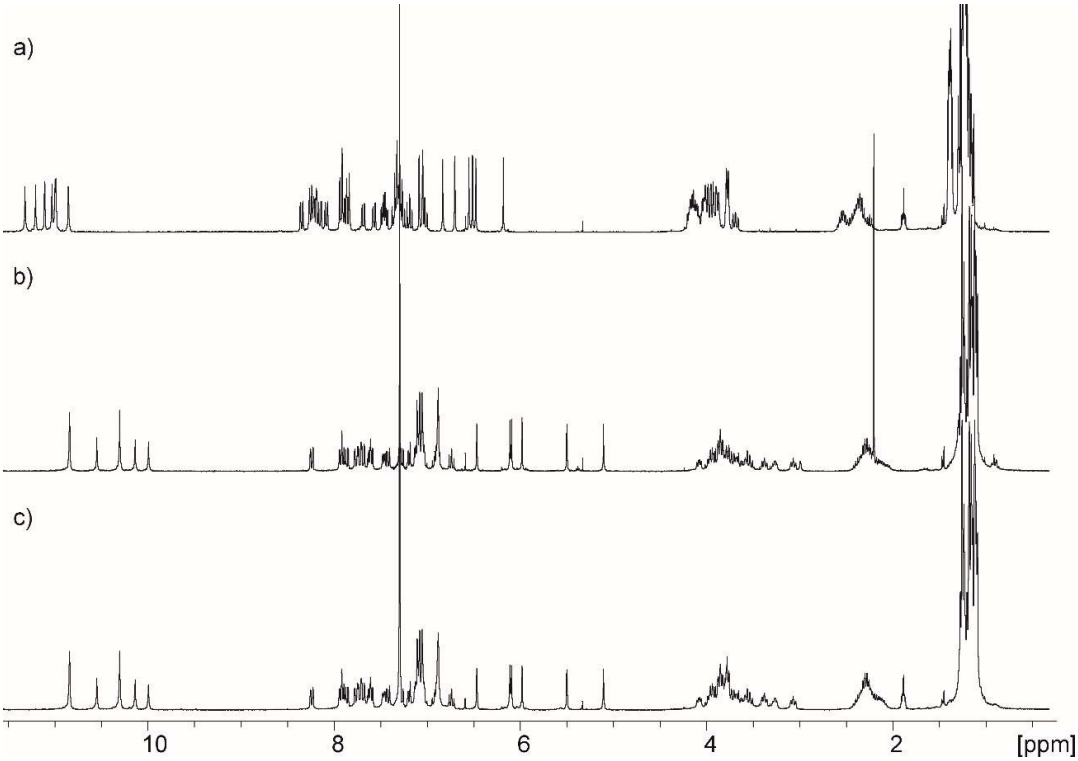

Figure S2. ^{1}H NMR spectra (300 MHz, 298K) of a $CDCl_3$ solution of a) Q_8-H b) Q_8-Na-Q_8 prepared by using aqueous NaOH (sat) c) Q_8-Na-Q_8 prepared by using NaOH powder

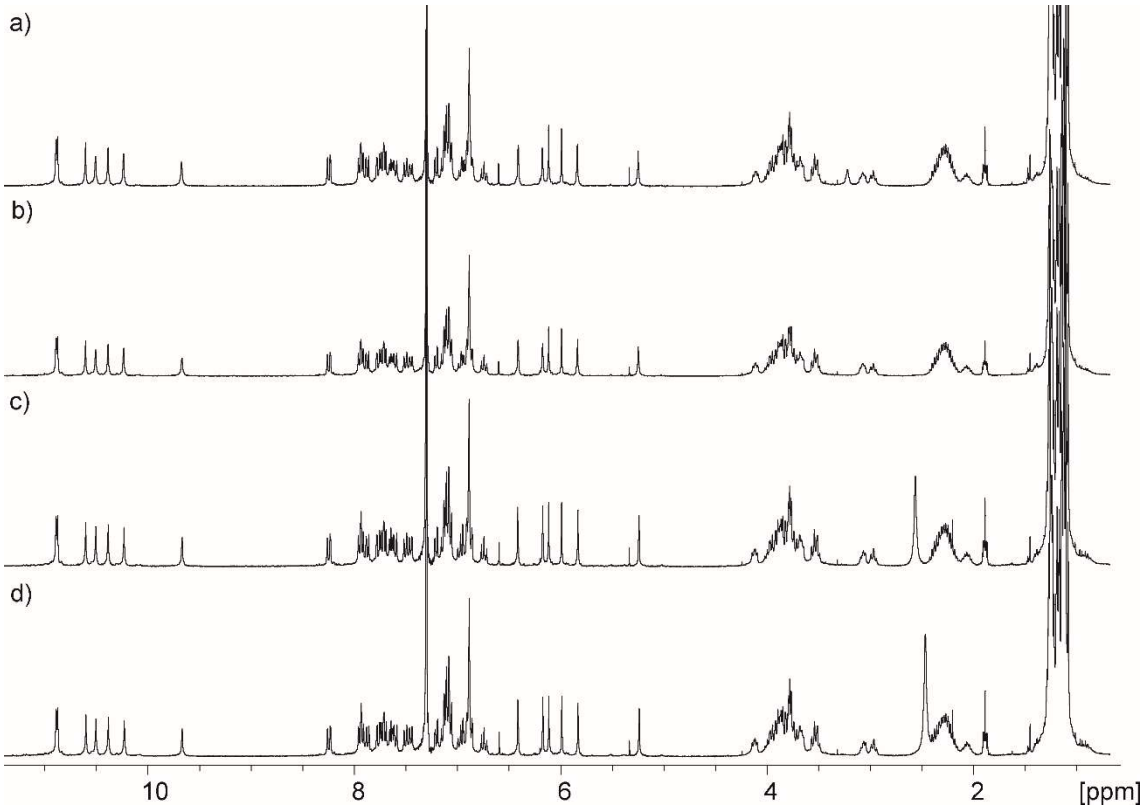

Figure S3. ^{1}H NMR spectra (300 MHz, 298K) of a $CDCl_3$ solution of Q_8-Na-Q_8 after a) 20 min b) 15h c) 2 days d) 5 days

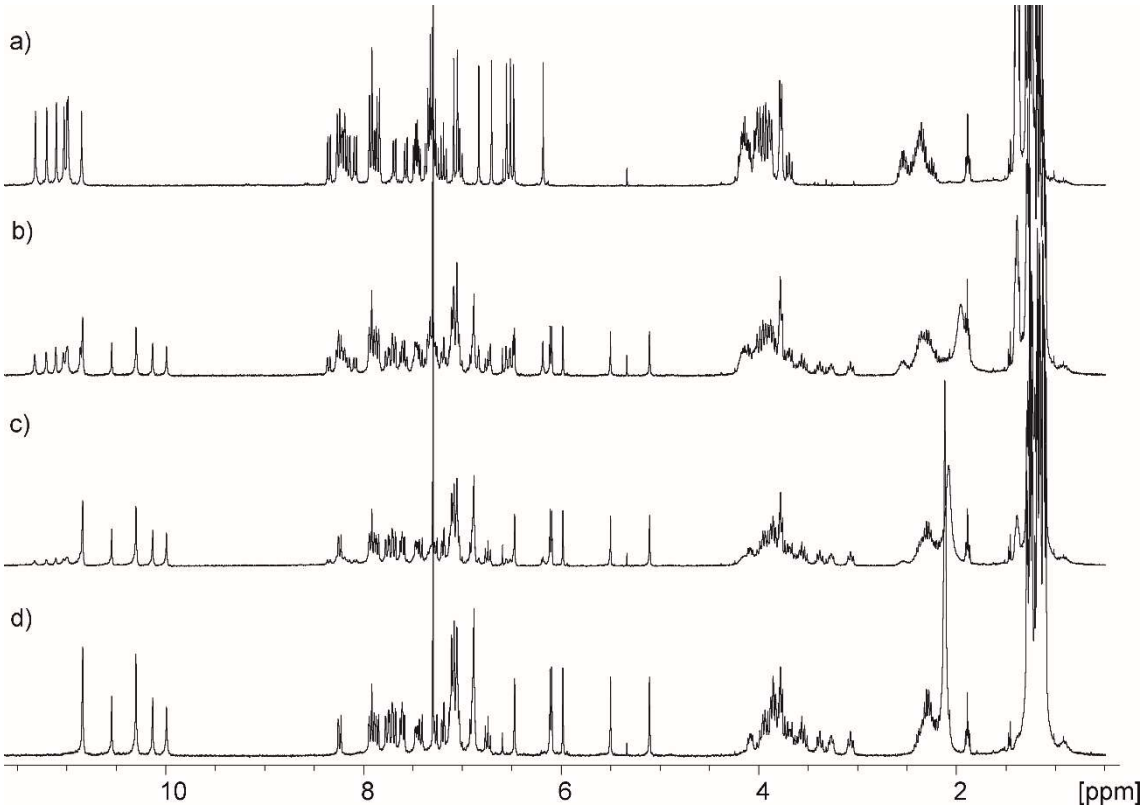

Figure S4. ^{1}H NMR spectra (300 MHz, 298K) of a $CDCl_3$ solution of a) Q_8-H b) Q_8-H and Na_2CO_3 powder after 15h c) 3 days d) 4 days

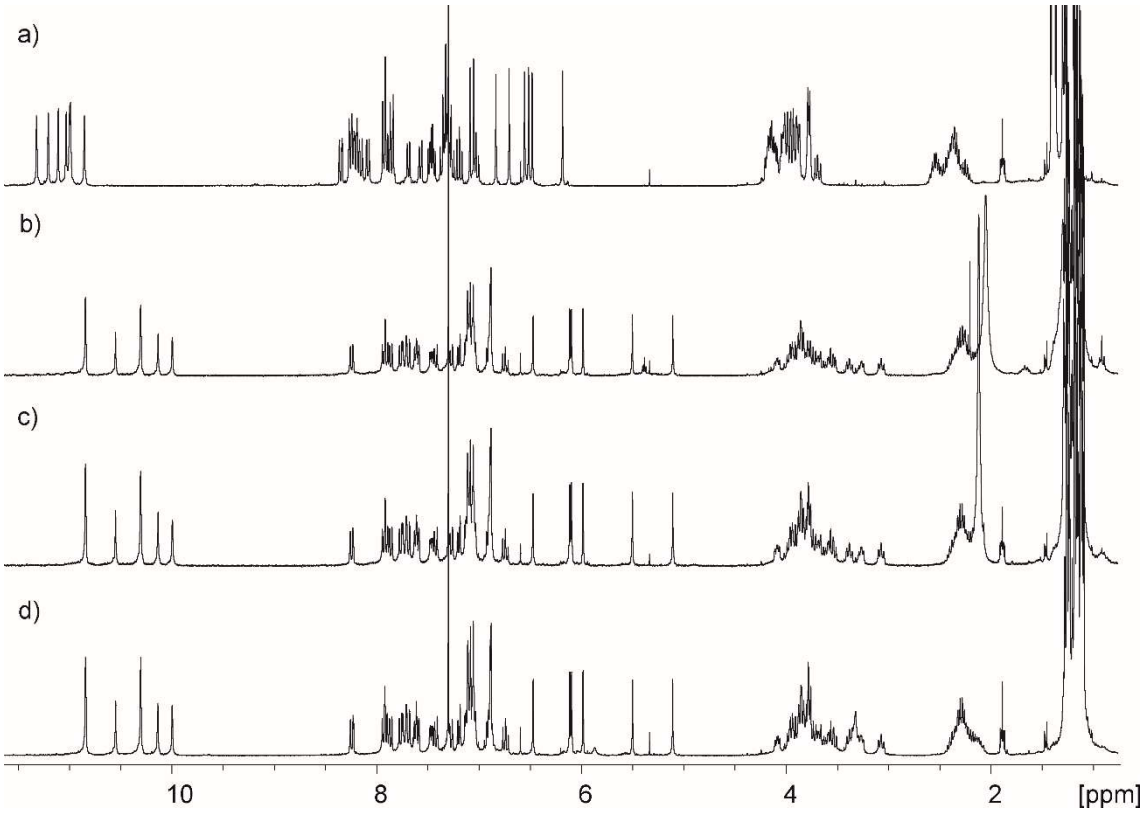

Figure S5. ^{1}H NMR spectra (300 MHz, 298K) of a $CDCl_3$ solution of a) Q_8-H b) Q_8-Na-Q_8 prepared by using aqueous Na_2CO_3 (sat) c) Q_8-Na-Q_8 prepared by using Na_2CO_3 powder after 4 days d) Q_8-Na-Q_8 prepared by using NaOH after 5 min

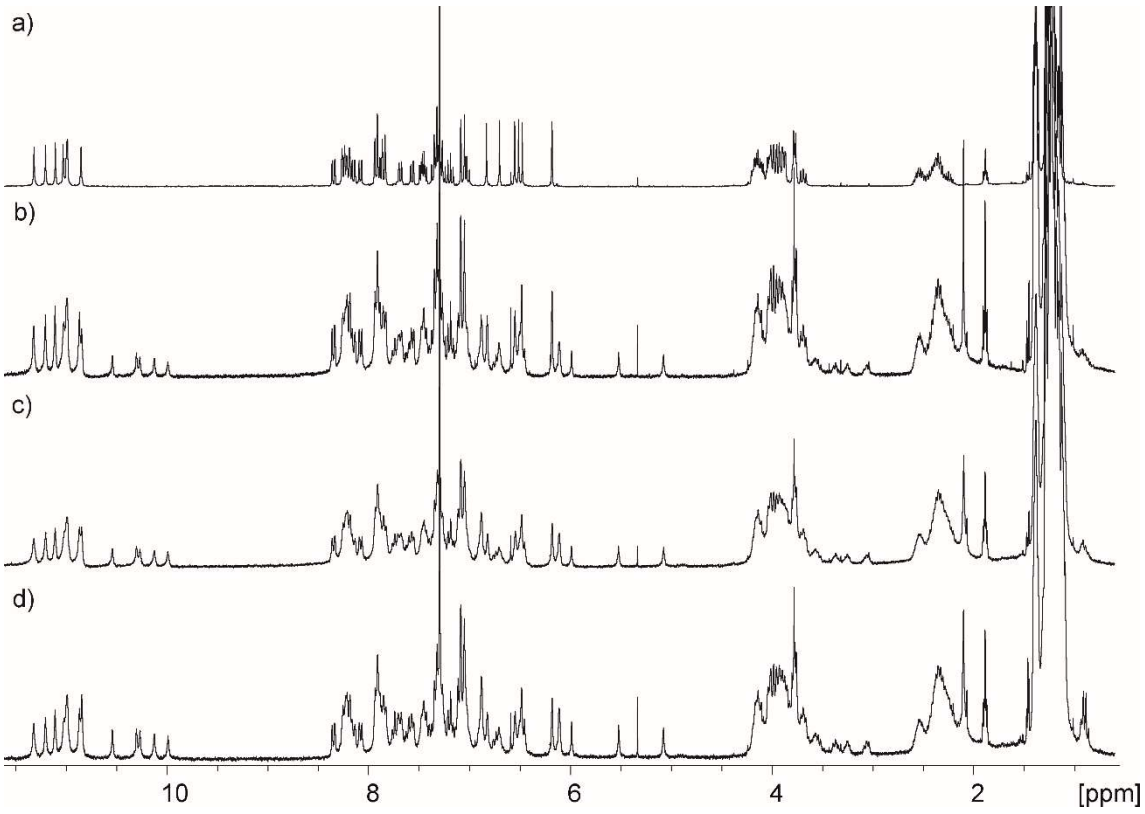

Figure S6. ^{1}H NMR spectra (300 MHz, 298K) of a $CDCl_3$ solution of a) Q_8-H b) Q_8-H and NaOAc powder after 2h c) 3 days d) 1 week

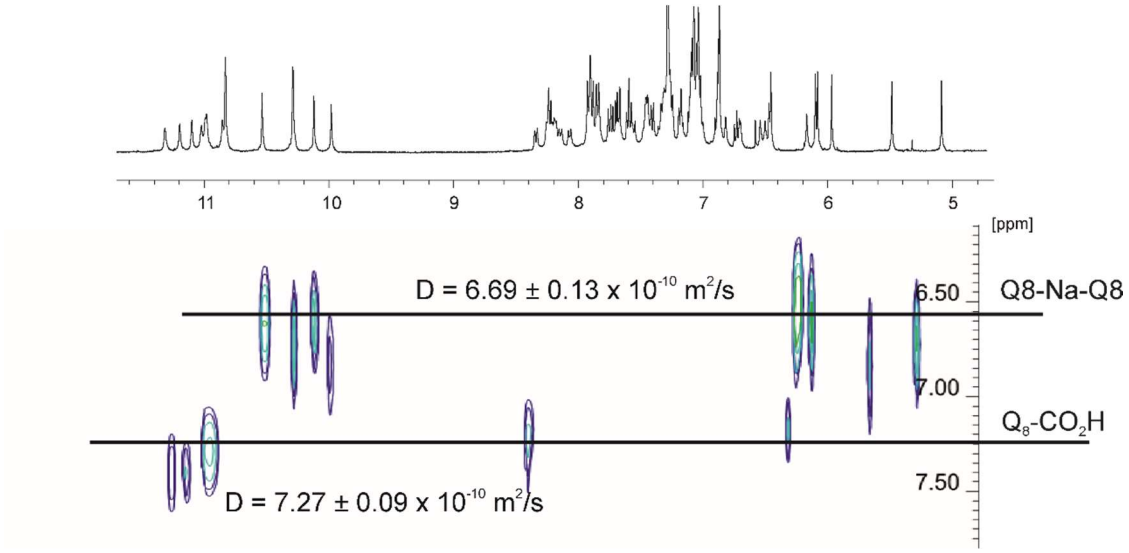

Figure S7. DOSY NMR (400 MHz, 298K) of a mixture of Q_8-H and Q_8-Na-Q_8. The exchange between the initial Q_8-H foldamer and the metal dimer is slow on the NMR time scale.

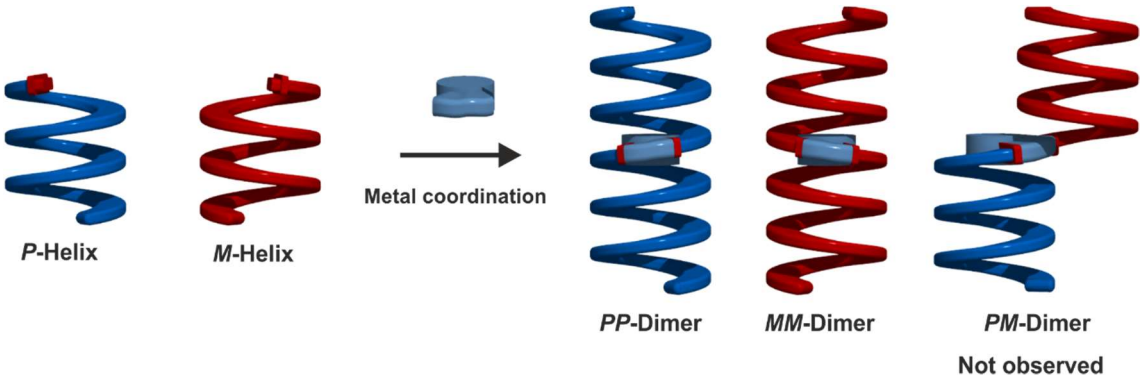

Figure S8. Schematic representation of the dimeric complex formation. A racemic mixture of P and M helices can form 3 species, PP, MM and PM dimers however only homochiral dimers are formed.

Potassium-ligated quinoline dimers:

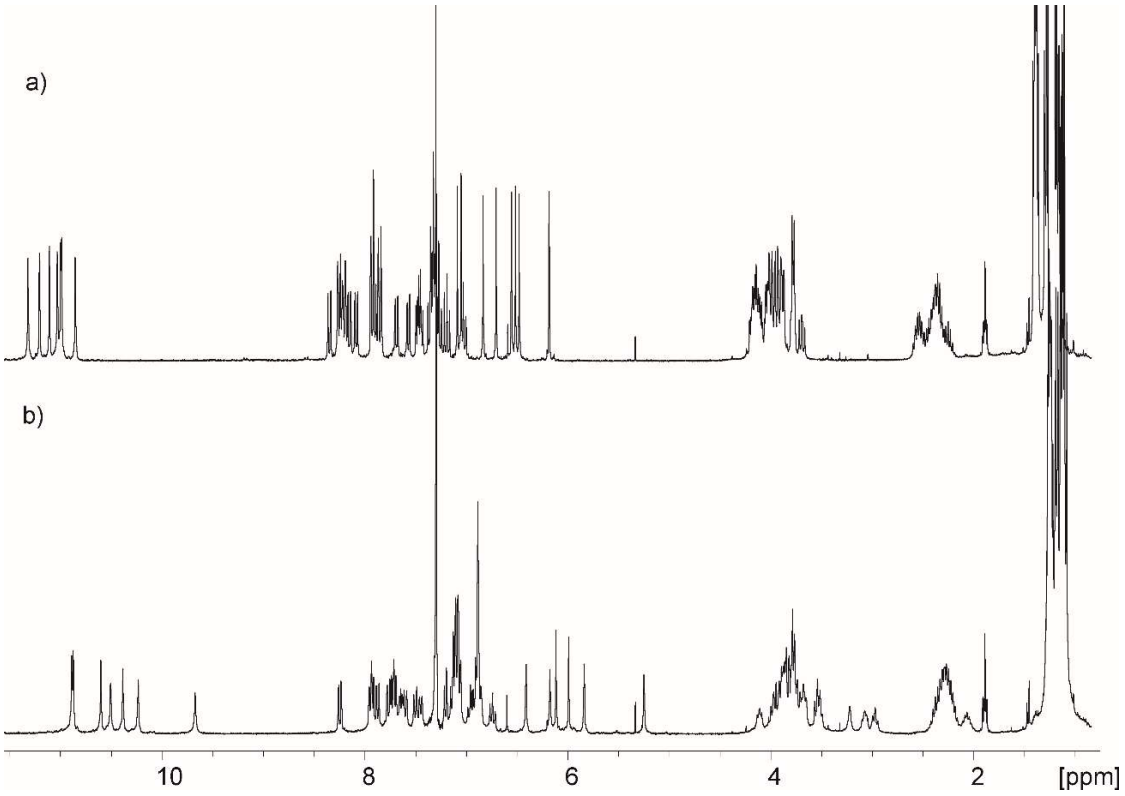

Figure S9. ^{1}H NMR spectra (300 MHz, 298K) of a $CDCl_3$ solution of a) Q_8-H b) Q_8-H and KOH powder after 5 min

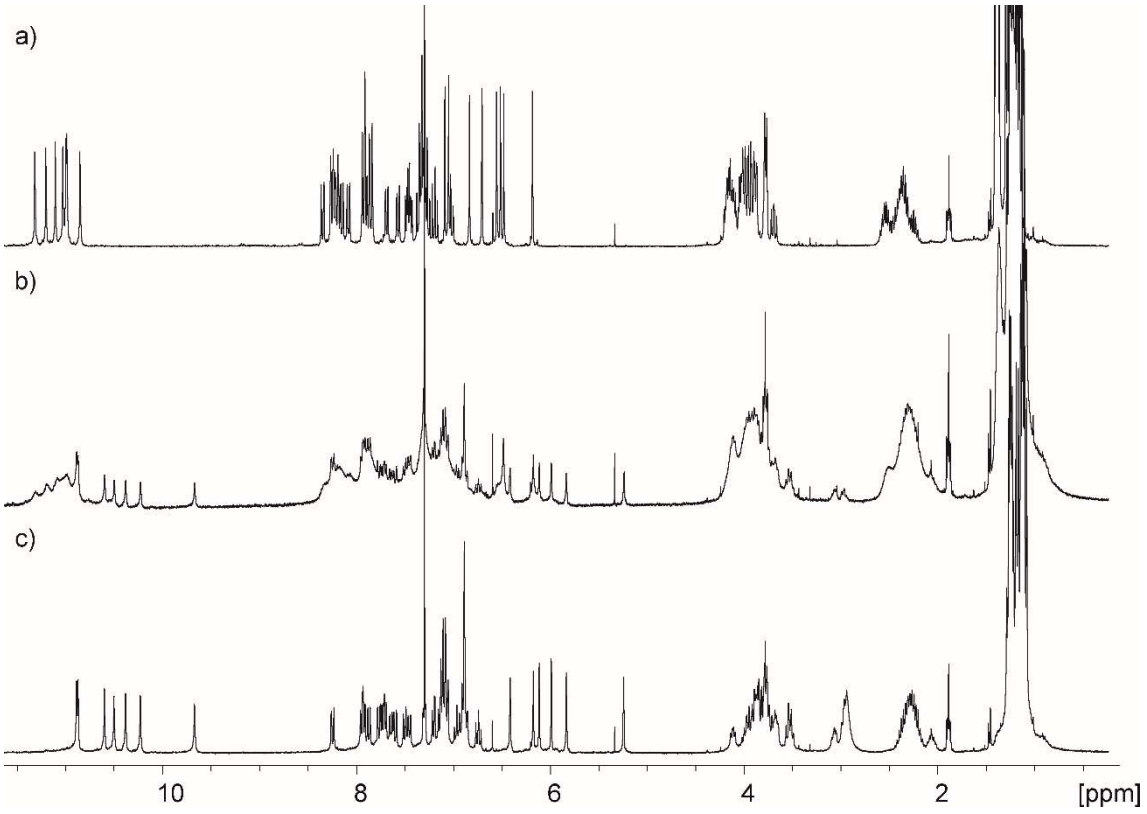

Figure S10. ^{1}H NMR spectra (300 MHz, 298K) of a $CDCl_3$ solution of a) Q_8-H b) Q_8-H and K_2CO_3 powder after 20 min c) 15h

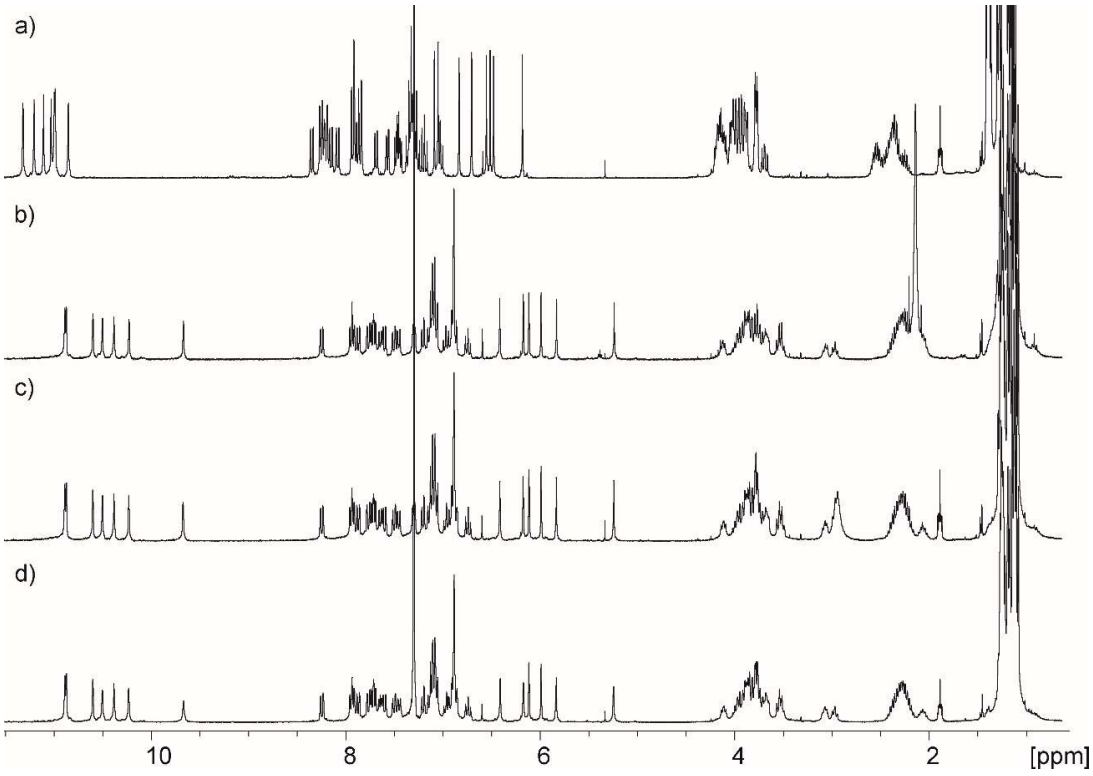

Figure S11. ^{1}H NMR spectra (300 MHz, 298K) of a $CDCl_3$ solution of a) Q_8-H b) Q_8-K-Q_8 prepared by using aqueous K_2CO_3 (sat) c) Q_8-K-Q_8 prepared by using K_2CO_3 powder d) Q_8-K-Q_8 prepared by using KOH

Lithium-ligated quinoline dimers:

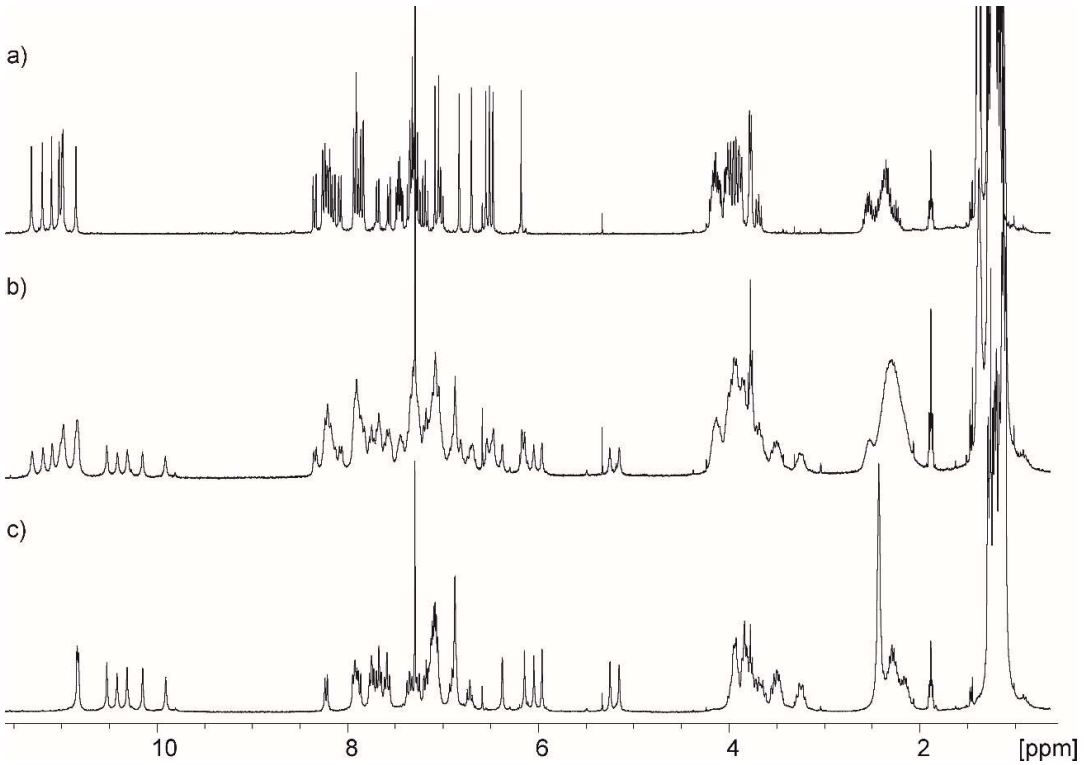

Figure S12. ^{1}H NMR spectra (300 MHz, 298K) of a $CDCl_3$ solution of a) Q_8-H b) Q_8-H and LiOH powder after 20 min c) 15h

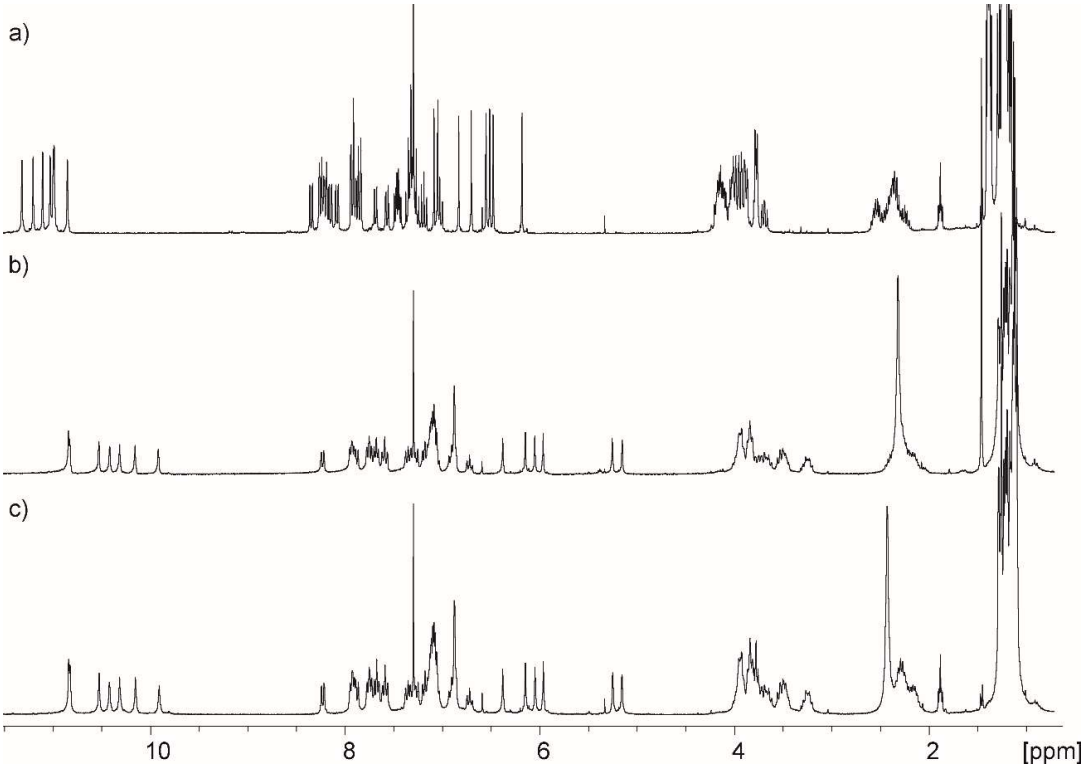

Figure S13. ^{1}H NMR spectra (300 MHz, 298K) of a $CDCl_3$ solution of a) Q_8-H b) Q_8-Li-Q_8 prepared by using aqueous LiOH (sat) c) Q_8-Li-Q_8 prepared by using LiOH powder

Silver-ligated quinoline dimers:

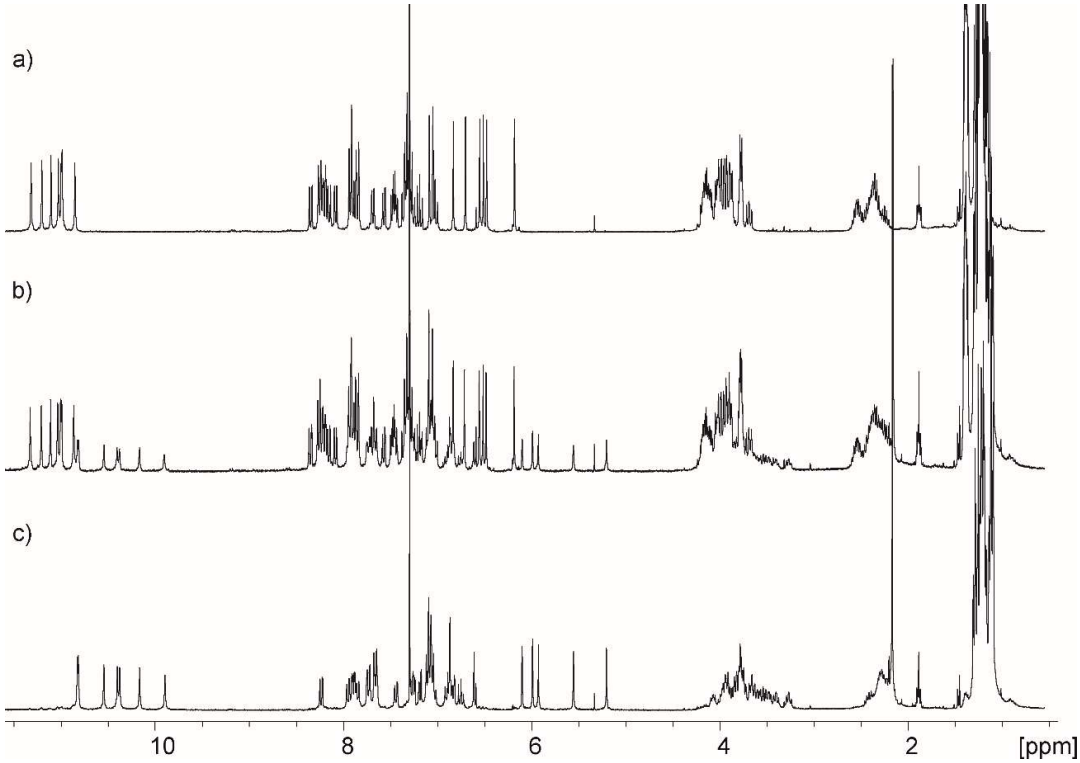

Figure S14. ^{1}H NMR spectra (300 MHz, 298K) of a $CDCl_3$ solution of a) Q_8-H b) Q_8-H and AgOAc powder after 1h c) 24h

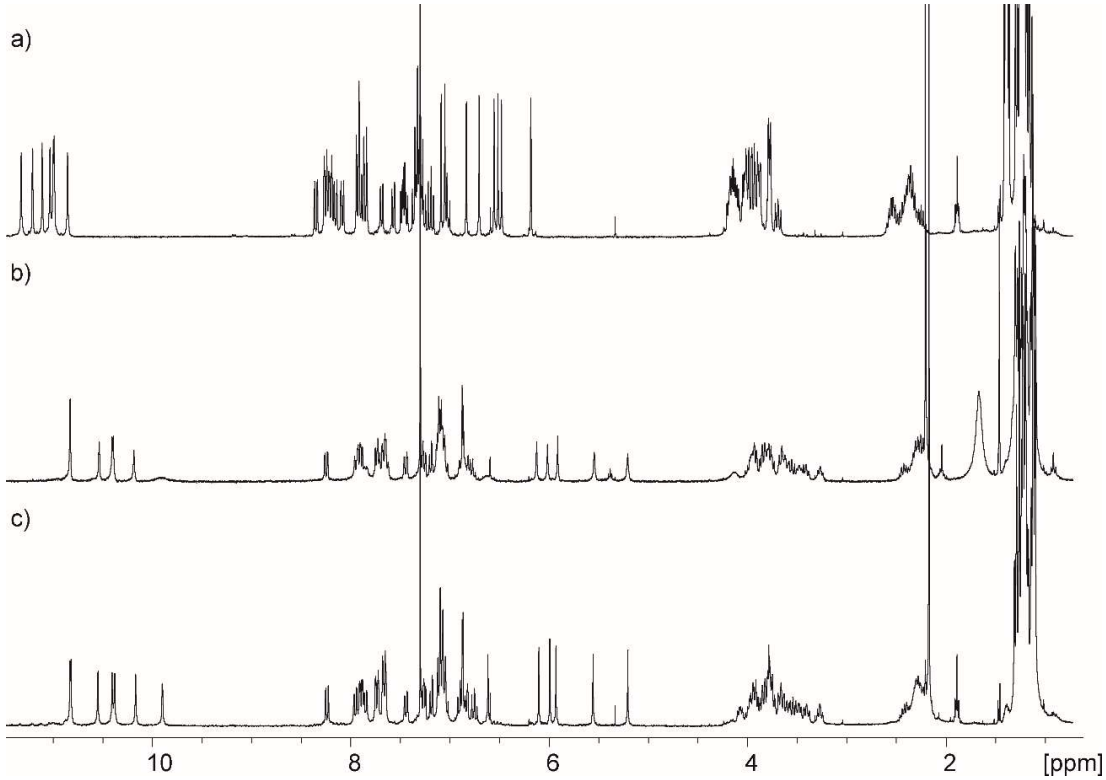

Figure S15. ^{1}H NMR spectra (300 MHz, 298K) of a $CDCl_3$ solution of a) Q_8-H b) Q_8-Ag-Q_8 prepared by using aqueous AgOAc (sat) c) Q_8-Ag-Q_8 prepared by using AgOAc powder

Mercury-ligated quinoline dimers:

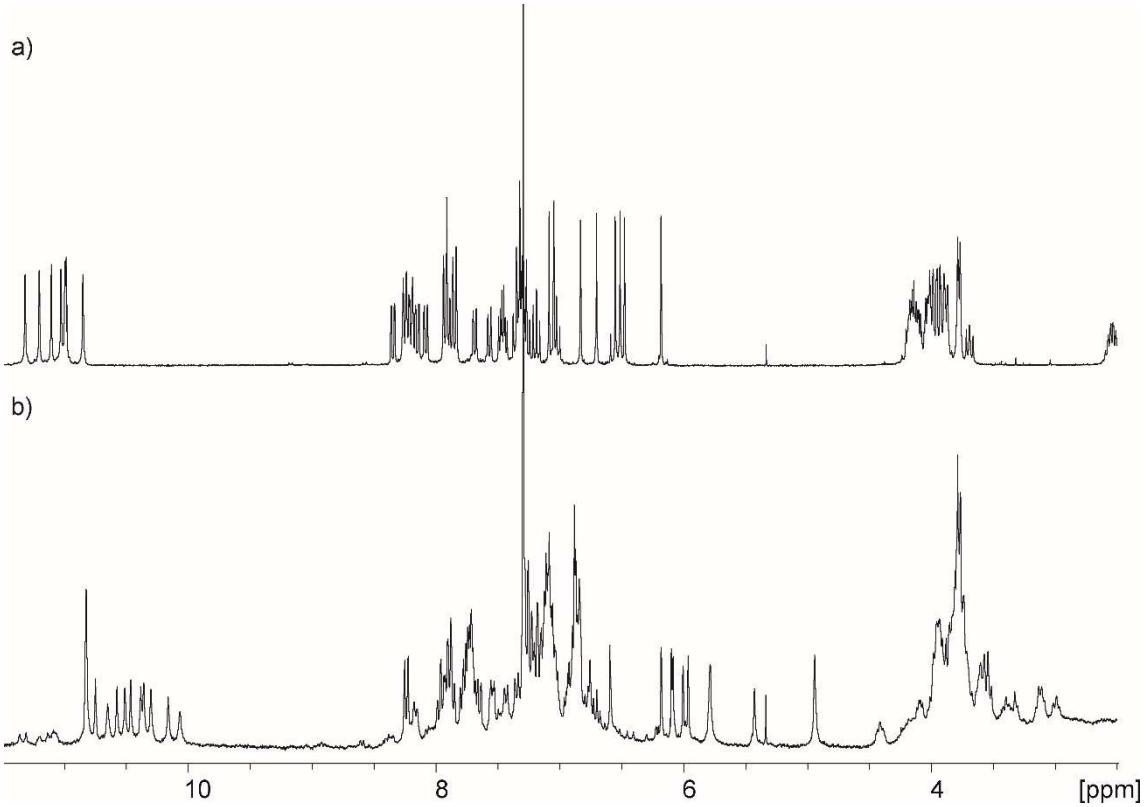

Figure S16. ^{1}H NMR spectra (300 MHz, 298K) of a $CDCl_3$ solution of a) Q_8-H b) Q_8-H and $Hg(OAc)_2$ powder after 5 min

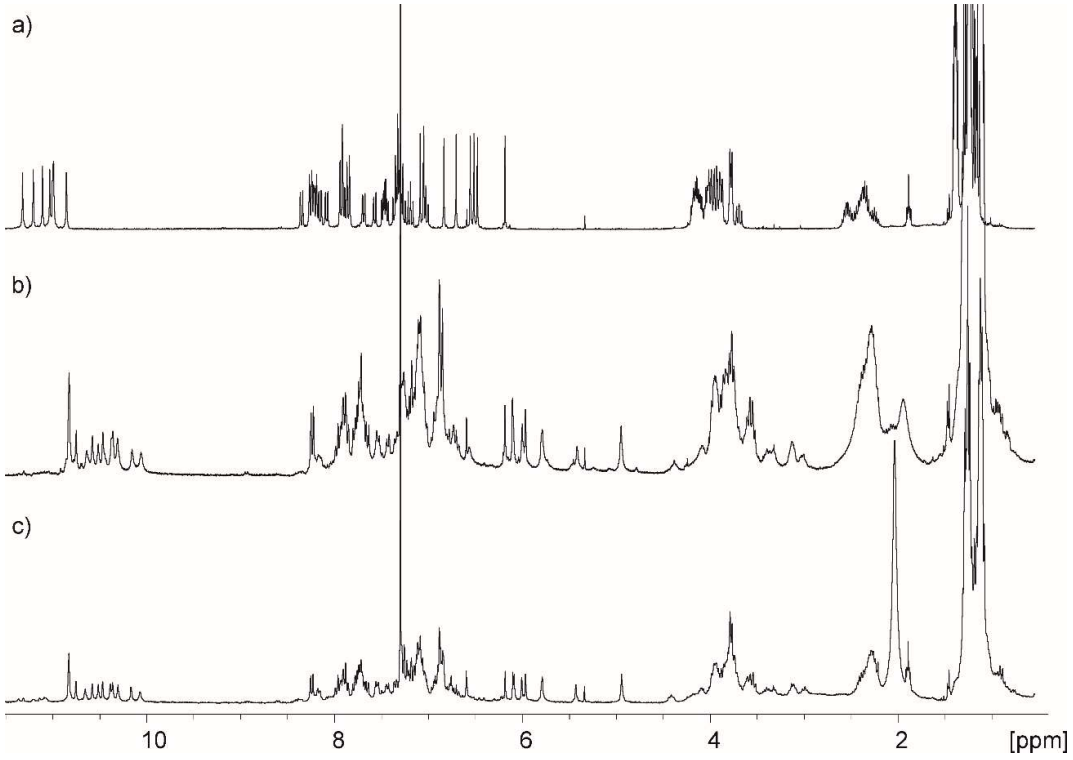

Figure 17. ^{1}H NMR spectra (300 MHz, 298K) of a $CDCl_3$ solution of a) Q_8-H b) Q_8-Hg-Q_8 prepared by using aqueous $Hg(OAc)_2$ (sat) c) Q_8-Hg-Q_8 prepared by using $Hg(OAc)_2$ powder

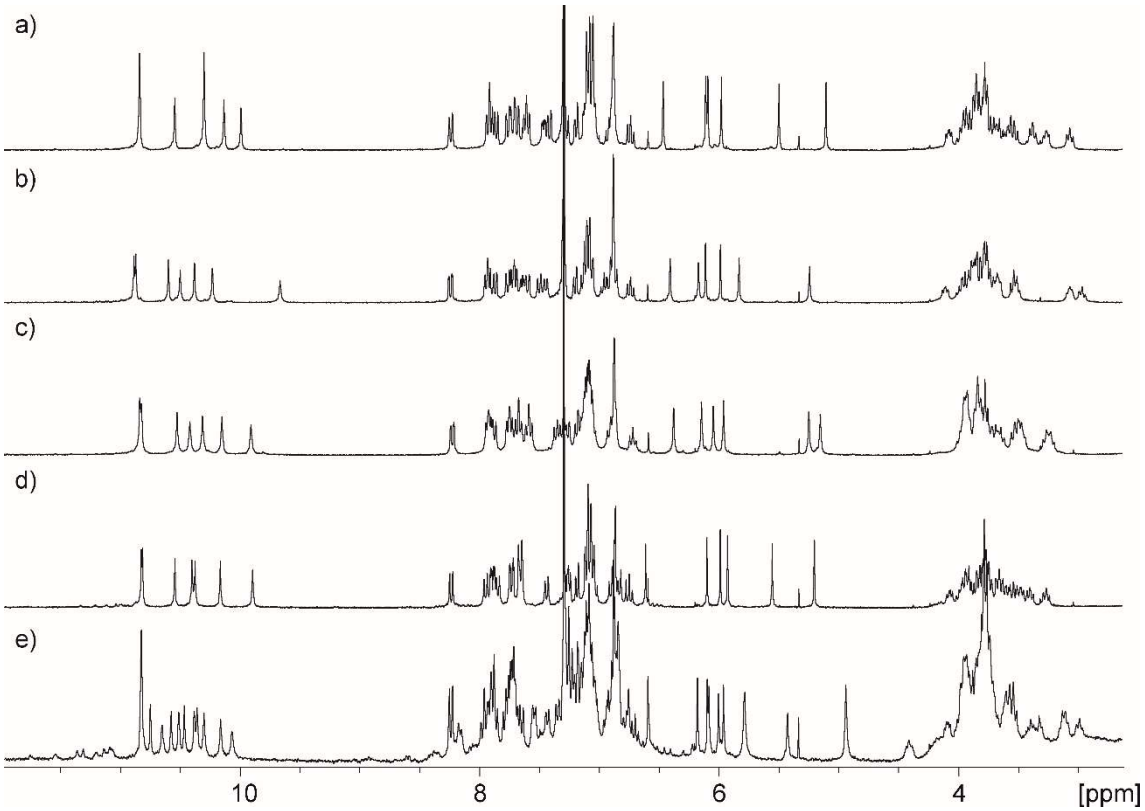

Figure S18. ^{1}H NMR spectra (300 MHz, 298K) of a $CDCl_3$ solution of a) Q_8-Na-Q_8 b) Q_8-K-Q_8 c) Q_8-Li-Q_8 d) Q_8-Ag-Q_8 e) Q_8-Hg-Q_8

Competitive experiments with different cations

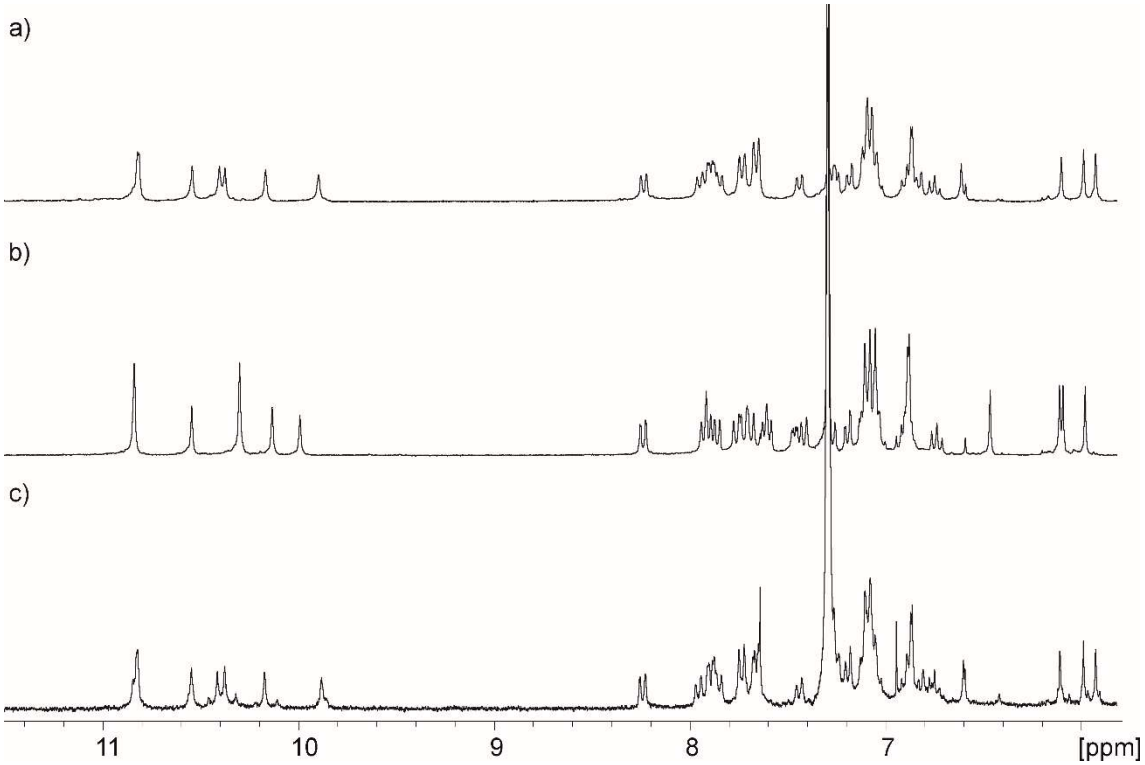

Figure S19. ^{1}H NMR spectra (300 MHz, 298K) of a $CDCl_3$ solution of a) Q_8-Ag-Q_8 b) Q_8-Na-Q_8 c) mixture of Q_8-H with equimolar amounts of NaOH and AgOAc

Very weak signals corresponding to Q_8-Na-Q_8 could be detected upon mixing Q_8-H with NaOH and AgOAc (Figure S19c), evidencing that the silver complex is more stable thermodynamically ($K_{Ag} > 100\ K_{Na}$). However, integration was hampered by the weak intensity of these signals and overlapping

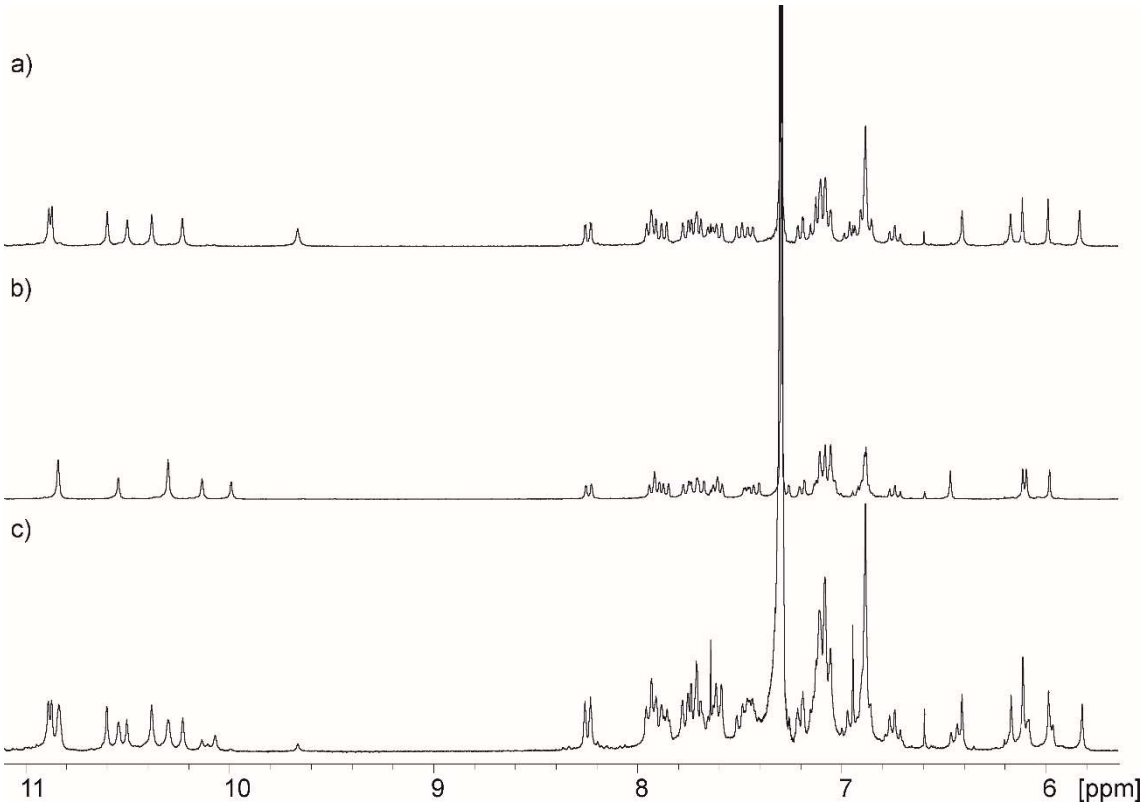

Figure S20. ^{1}H NMR spectra (300 MHz, 298K) of a $CDCl_3$ solution of a) Q_8-K-Q_8 b) Q_8-Na-Q_8 c) mixture of Q_8-H with equimolar amounts of NaOH and KOH

The mixing of Q_8-H with NaOH and KOH produces both complexes: Q_8-K-Q_8 and Q_8-Na-Q_8. By integration, we can calculate and estimate a ratio of association constants such as $K_{Na} = 1.25\ K_K$

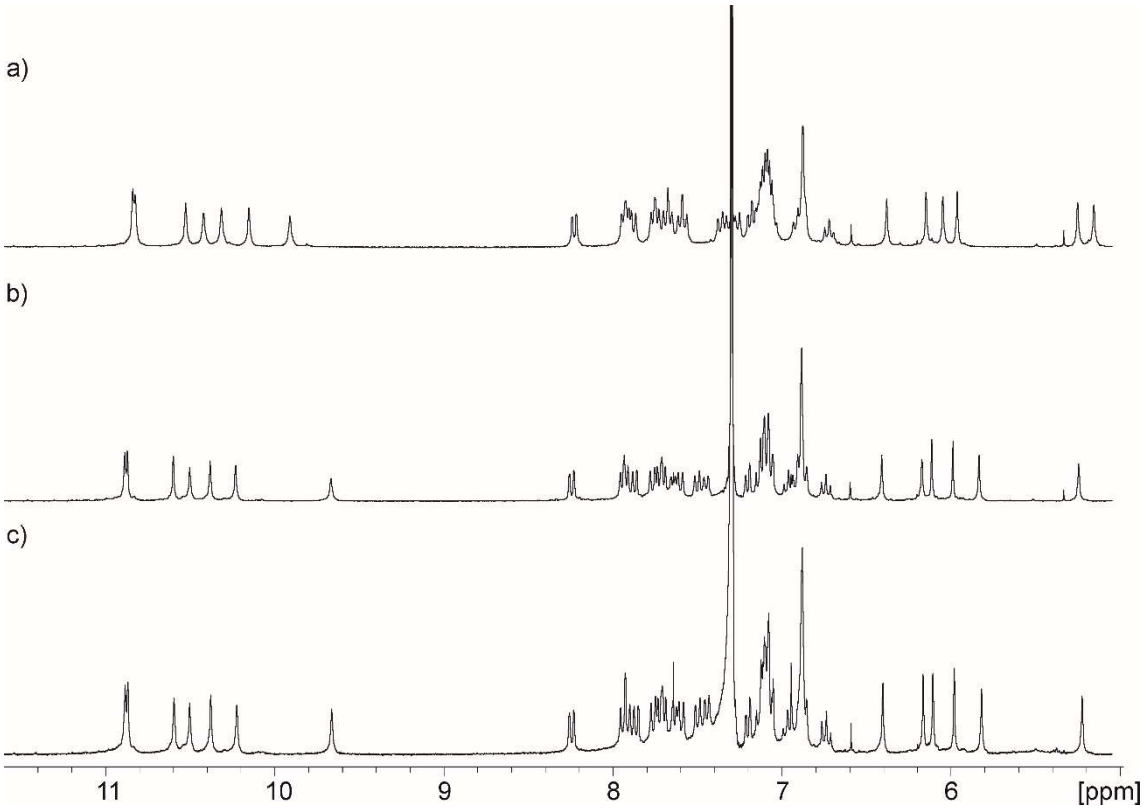

Figure S21. ^{1}H NMR spectra (300 MHz, 298K) of a $CDCl_3$ solution of a) Q_8-Li-Q_8 b) Q_8-Na-Q_8 c) mixture of Q_8-CO_2H with equimolar amounts of LiOH and KOH

Mixing Q_8-H with LiOH and KOH produces the Q_8-K-Q_8 complex exclusively (Figure S21c) evidencing that $K_K > 100\ K_{Li}$

Conclusion: Competitive pairwise experiments performed between the different salts showed that the order of thermodynamic stability of the complexes is as follows: Ag > Na > K > Li. The splitting of the signals when using mercury salt hinders its use in competitive experiments.

3. Dynamics of the complexes in solution: exchange experiments

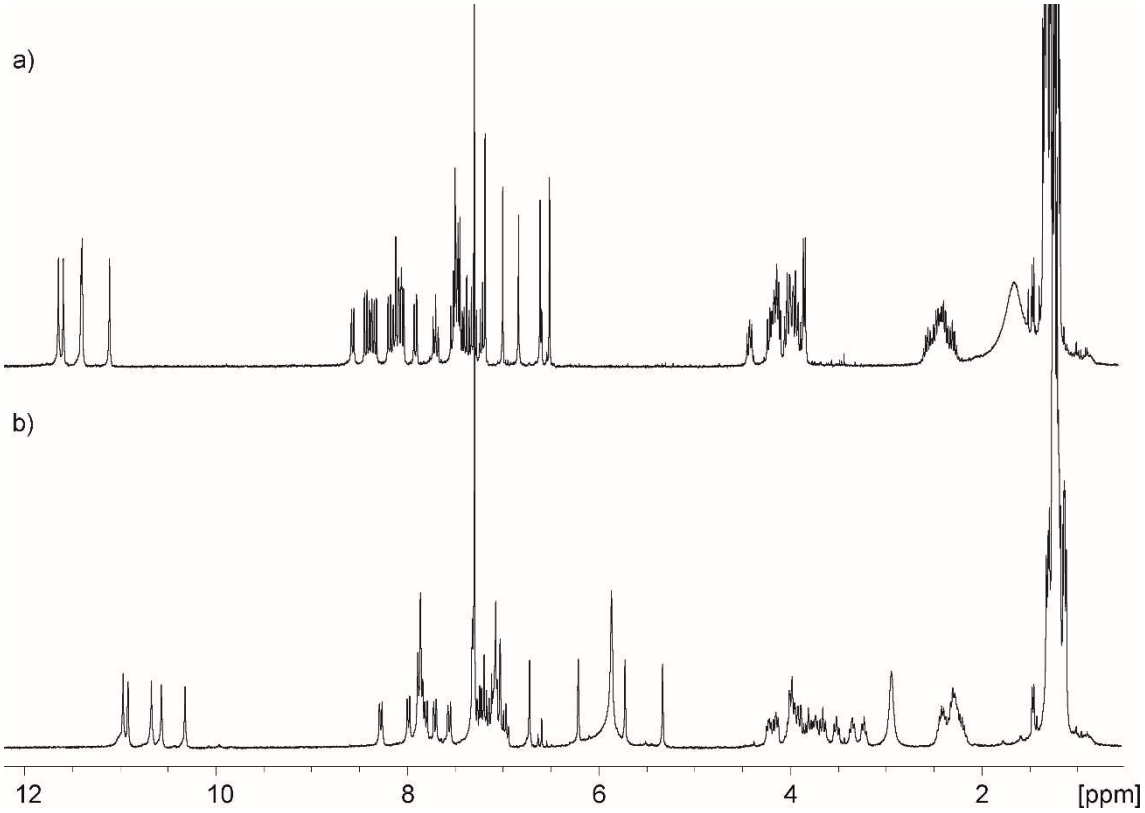

Figure S22. ^{1}H NMR spectra (300 MHz, 298K) of a $CDCl_3$ solution of a) Q_6-H b) Q_6-H and NaOH powder (Q_6-Na-Q_6)

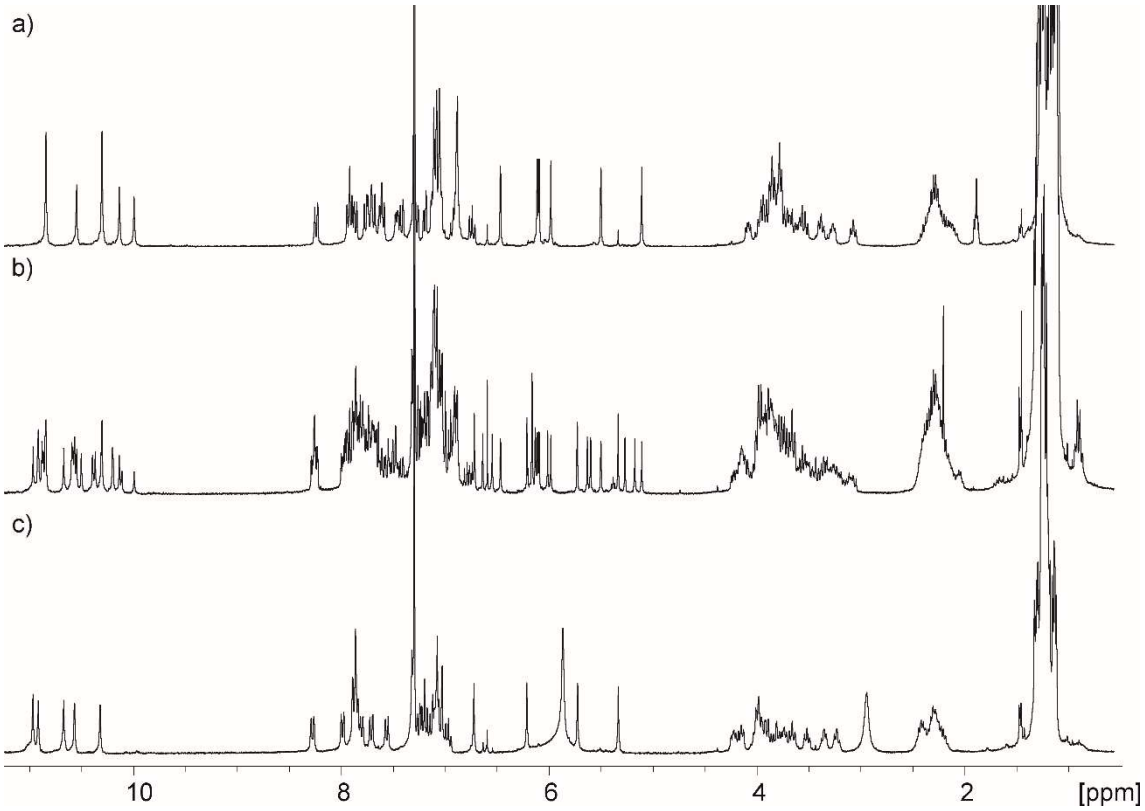

Figure S23. ^{1}H NMR spectra (300 MHz, 298K) of a $CDCl_3$ solution of a) Q_8-Na-Q_8 b) an equimolar mixture of Q_8-Na-Q_8 and Q_6-H in the presence of NaOH excess c) Q_6-Na-Q_6

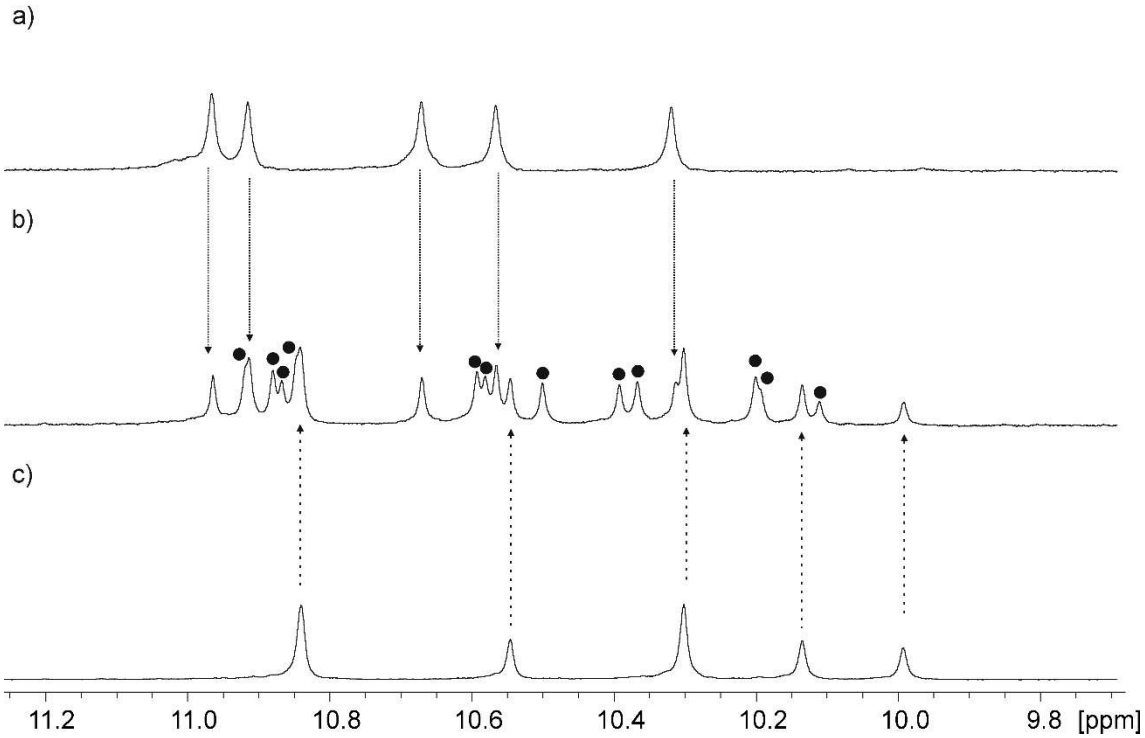

Figure S24. Downfield region (amide NHs) of ^{1}H NMR spectra (300 MHz, 298K) of a $CDCl_3$ solution of a) Q_6-Na-Q_6 b) an equimolar mixture of Q_8-Na-Q_8 and Q_6-H in the presence of NaOH excess c) Q_8-Na-Q_8. Protons from heterodimer Q_8-Na-Q_6 are marked with a black dot

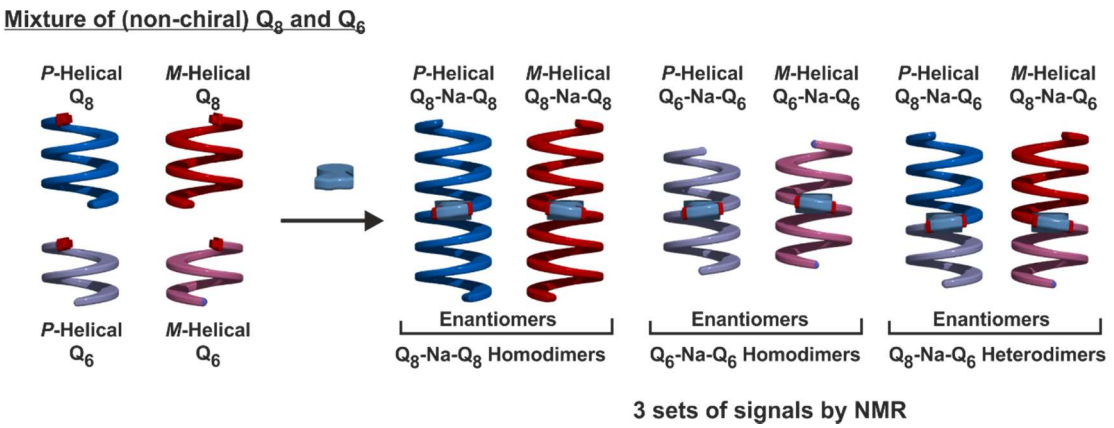

Figure S25. Schematic representation of dimers formation, using a mixture of non-chiral Q8 and Q6. Both oligomers give right and left handed helices which self-assembled though metal coordination with helices of similar handedness giving rise to 3 pairs of enantiomers.

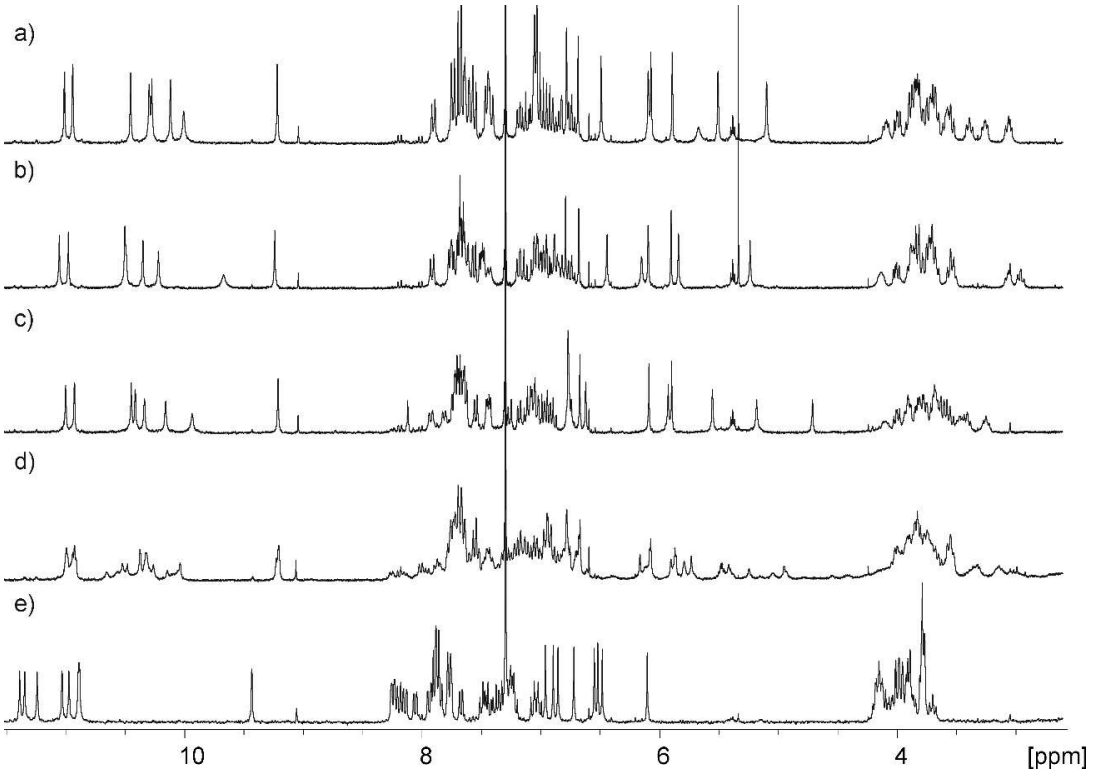

Figure S26. ^{1}H NMR spectra (300 MHz, 298K) of a $CDCl_3$ solution of b) *R*-Q_8-Na-*R*-Q_8 b) *R*-Q_8-K-*R*-Q_8 c) *R*-Q_8-Ag-*R*-Q_8 d) *R*-Q_8-Hg-*R*-Q_8 e) *R*-Q_8-H

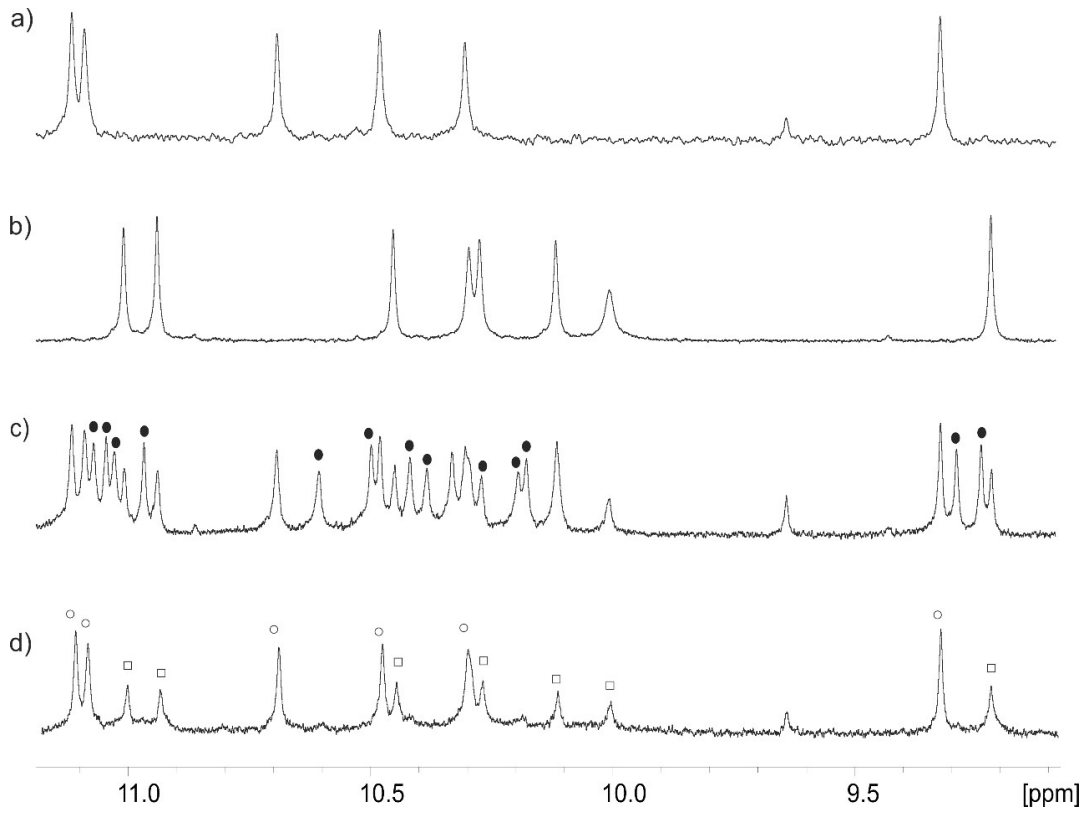

Figure S27. Downfield region (amide NHs) of ^{1}H NMR spectra (300 MHz, 298K) of a CDCl3 solution of a) S-Q6-Na-S-Q6 b) R-Q8-Na-R-Q8; c) mixture of S-Q8-H and S-Q6-H in the presence of NaOH excess, peaks from heterodimer *S*-Q_6-Na-*S*-Q_8 are marked with black dots. d) mixture of *R*-Q_8-H and *S*-Q_6-H in the presence of NaOH in excess, peaks from homodimer *S*-Q_6-Na-*S*-Q_6 are marked with white dots. Peaks from homodimer *R*-Q_8-Na-*R*-Q_8 are marked with white squares.

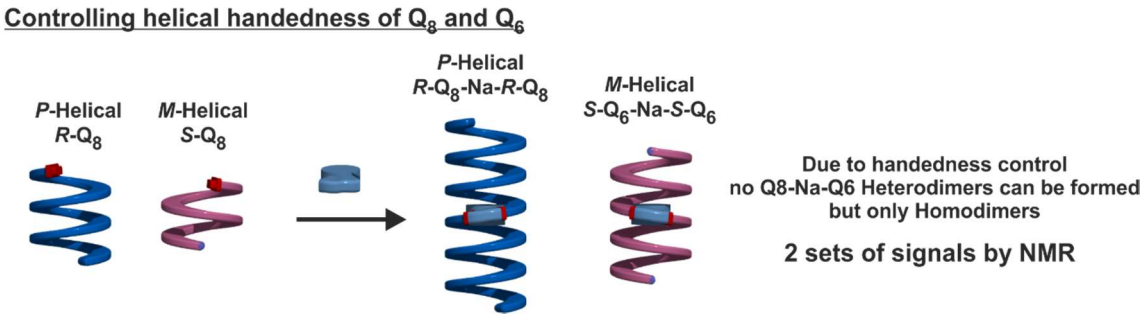

Figure S28. Schematic representation of dimers formation, using a mixture of chiral R-Q8 and S-Q6 that fold into helices of opposite handedness. Though metal coordination only helices of similar handedness can self-assembled, allowing only the formation of homodimers.

4. Characterization of the complexes in the solid-state

Single crystals used for X-ray diffraction experiments were obtained by diffusion of n-hexane to a chloroform solution of the dimer through a dichloromethane buffer solution in the case of **Q_8-K-Q_8**, to a filtered solution of the complex in chloroform for **Q_8-Na-Q_8**, and dichloromethane solution for **Q_8-Hg-Q_8**. The diffraction data were collected at the IECB x-ray facility (CNCR AUR 3033 – INSERM US001) with a Rigaku FRX rotating anode (2.9 kW) diffractometer. CuKα radiation monochromated with high flux Osmic Varimax HF mirrors was used for data collection. The x-ray source was equipped with a Dectris Pilatus 200K detector and a partial chi goniometer. All crystals were kept at 100(2) K during data collection. The data were processed with the Rigaku CrystalClear suite[1] with a multiscan absorption correction. Structures were solved with the ShelXT[2] structure solution program using a dual-space algorithm. Crystal model refinement was performed with ShelXL[3] package using the Least Squares minimization implemented in Olex2[4].

The resolution of the data diffraction is lower than expected for medium size molecules due to the characteristics of the crystals, large volume fractions of disordered solvent molecules, instability after removing from the mother liquor, and disorder of side chains. Additionally, crystals of the **Q_8-Na-Q_8** complex decomposed during data collection, causing not only limited resolution of the data (Figure SX) but also elevated R_{int} and refining factors.

Anisotropic displacement parameters were used during refinement for backbones and some coordinated solvent molecules. In the case of **Q_8-K-Q_8**, the anisotropic model was also introduced for some of the isobutyl side chains. Other non-hydrogen atoms were refined with isotropic approximation. Due to the high uncertainty of the positions of side chains and solvent molecules, the positions of hydrogen atoms were not calculated. However, those atoms participate in the X-ray diffraction, so they are introduced in the SFAC calculations. Hydrogen atoms of quinoline rings and amide N-H groups were placed at an idealized position and were refined in the riding-model approximation, with $U_{iso}(H)=1.2U_{eq}(CH, NH)$. EADP and DELU instructions were employed to model temperature parameters. The geometry of the molecules was improved with DFIX and AFIX commands.

In the structures, wide channels (**Q_8-K-Q_8**, **Q_8-Hg-Q_8**) or large voids (**Q_8-Na-Q_8**) occupying about 12% (**Q_8-K-Q_8**), 24% (**Q_8-Hg-Q_8**) and 11% (**Q_8-Na-Q_8**) of the unit cell volume are formed. These spaces are filled with severely disordered solvent molecules, which during refinement, were removed using a solvent mask procedure implemented in Olex2[9]. The solvent radius was set to 1.2 Å, and calculated total potential solvent-accessible void volume and electron counts per unit-cell were: 3372 $Å^3$ and 640 for **Q_8-Na-Q_8**, 1759 $Å^3$ and 280 for **Q_8-K-Q_8**, 6928 $Å^3$ and 1169 **Q_8-Hg-Q_8**. Considering the high number of electrons calculated for the channels or voids and the variety of solvents used for crystallization, it is impossible to determine the solvent composition reliably. However, structure factors include contributions from the .fab file.

The final cif files were checked using IUCR's checkcif algorithm. Due to the characteristics of the crystals mentioned above, A-level and B-level alerts remain in the checkcif file. These alerts are inherent to the data and refinement procedures and do not reflect errors. They are explicitly listed below and have been divided into two groups.

Group 1:

THETM01_ALERT_3_A, B The value of sine(theta_max)/wavelength is less than 0.550 or 0.575

PLAT023_ALERT_3_A, B Resolution (too) Low [sin(theta)/Lambda < 0.6]

PLAT029_ALERT_3_B _diffrn_measured_fraction_theta_full value Low

PLAT082_ALERT_2_A, B High R1 Value

PLAT084_ALERT_3_A High wR2 Value (i.e. > 0.25)

PLAT220_ALERT_2_B NonSolvent Resd 1 C Ueq(max)/Ueq(min) Range 9.0 Ratio

PLAT230_ALERT_2_B Hirshfeld Test Diff

PLAT234_ALERT_4_B Large Hirshfeld Difference

PLAT241_ALERT_2_B High 'MainMol' Ueq as Compared to Neighbors

PLAT242_ALERT_2_B Low 'MainMol' Ueq as Compared to Neighbors

PLAT340_ALERT_3_B Low Bond Precision on C-C Bonds

PLAT934_ALERT_3_B Number of (Iobs-Icalc)/Sigma(W) > 10 Outliers

Group 2:

PLAT201_ALERT_2_A Isotropic non-H Atoms in Main Residue(s)

As mentioned above, not all atoms were refined with ADPs

PLAT306_ALERT_2_B Isolated Oxygen Atom (H-atoms Missing ?)

PLAT315_ALERT_2_B Singly Bonded Carbon Detected (H-atoms Missing)

As mentioned above, not all H-atoms were localized

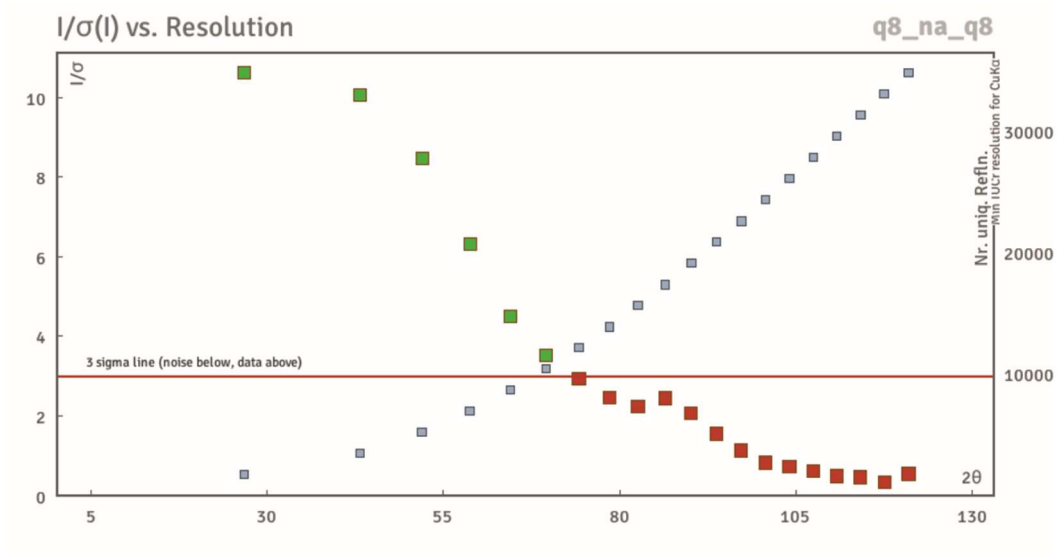

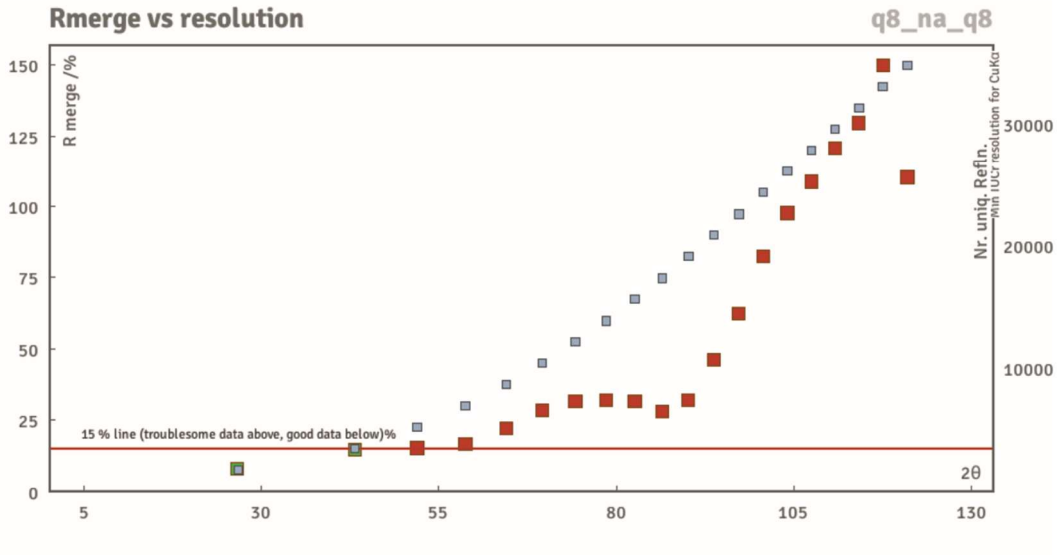

Figure S29: I/σ(i) and R_{merge} versus resolution graphs showing limited resolution of the data for **Q_8-Na-Q_8**.

[1] CrystalClear-SM Expert 2.1 (*Rigaku* 2013) Software, Version 5.6.2.0, Tokyo, Japan.

[2] G. M. Sheldrick, *Acta Cryst.* **2015**, *A71*, 3–8.

[3] G. M. Sheldrick, *Acta Cryst.* **2015**, C71, 3-8.

[4] O.V. Dolomanov, L.J . Bourhis, R.J . Gildea, J.A.K. Howard, H. Puschmann, *J. Appl. Cryst.* **2009**, 42, 339-341.

Table S1. Crystal data and refinement details.

Identification code	**Q_8-Na-Q_8**	**Q_8-K-Q_8**	**Q_8-Hg-Q_8**
Chemical formula	$C_{225}H_{227}Cl_3N_{32}Na_2O_{40}$ 3($CHCl_3$) (solvent)*	$C_{224}H_{226}N_{32}K_2O_{40}$ (solvent)*	$C_{224}H_{225}HgKN_{32}O_{40}$·2($CH_2Cl_2$)· 2($H_2O$) (solvent)*
Formula weight	4529.81	4084.55	4450.92
Crystal system	Monoclinic	Triclinic	Monoclinic
Space group	$P2_1/c$	P-1	$C2/c$
Unit cell dimensions (Å, °)	a=44.863 (14), α=90	a=19.053 (4), α=66.46 (1)	a=43.956 (8), α=90
	b=19.062 (5), β=106.137 (7)	b=24.368 (4), β=88.27 (2)	b=18.100 (3), β=111.362 (3)
	c=28.749 (9), γ=90	c=26.337 (5), γ=80.27 (2)	c=34.426 (6), γ=90
Volume (Å^3)	23617 (12)	11040 (4)	25508 (7)
Z	4	2	4
Density (calculated) (Mg m^{-3})	1.274	1.229	1.159
Absorption coefficient (mm^{-1})	1.96	1.03	2.19
Crystal size (mm)	0.20 × 0.08 × 0.03	0.30 × 0.20 × 0.01	0.30 × 0.10 × 0.02
Completeness	94.8 (up to 50.43°)	98.0 (up to 58.94°)	99.0 (up to 51.87°)
Reflections collected	90366	117829	55703
Reflections observed [$I > 2\sigma(I)$]	13209	13719	9509
R_{int}	0.126	0.086	0.087
Data/parameters/restrains	23448/1888/358	31068/2549/44	14057/1113/93
Goodness-of-fit on F^2	1.67	1.01	1.32
Final R indices [$I > 2\sigma(I)$]	0.1931, 0.4720	0.0989, 0.2756	0.1192, 0.3478
R indices (all data)	0.2416, 0.5113	0.1804, 0.3316	0.1406, 0.3589
Largest diff. peak and hole	1.08, -0.79	0.91, -0.47	1.20, -0.92
CCDC #	2194086	2194087	2194085

* Solvent mask was used to remove severely disordered solvent molecules.

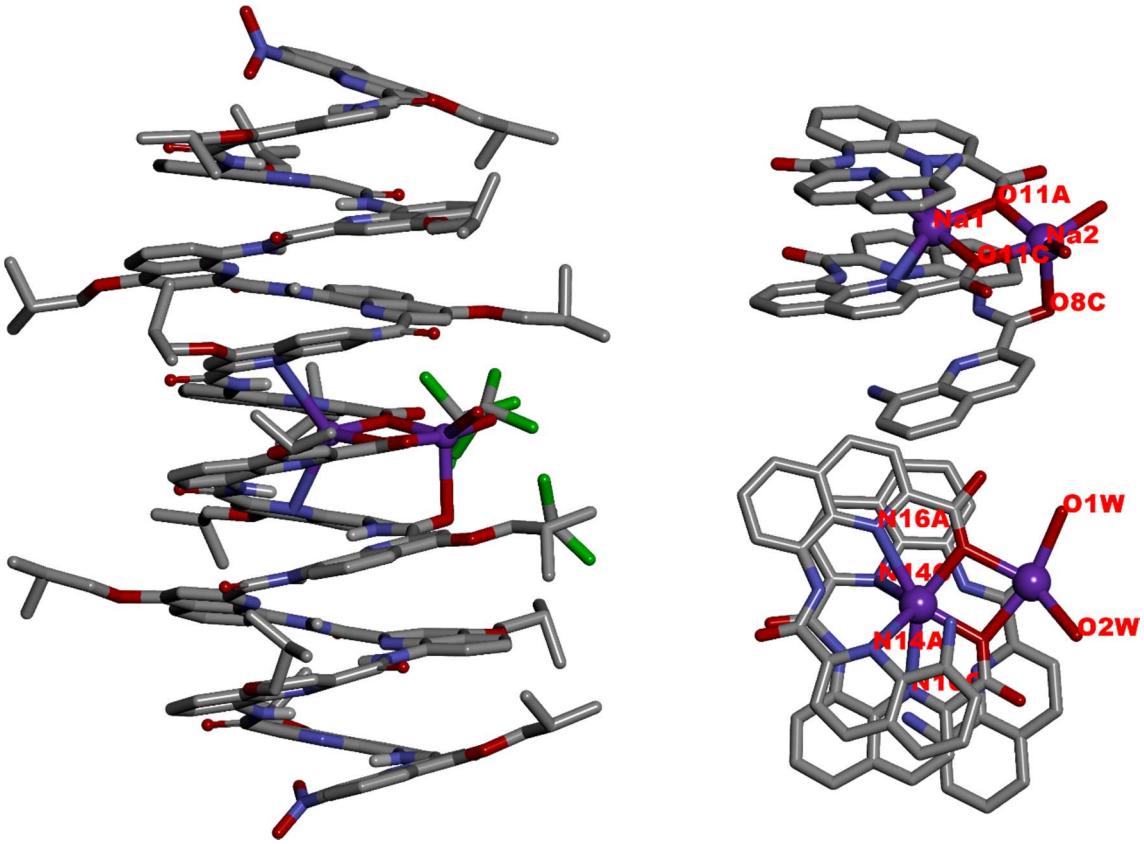

Figure S30: X-ray structures of the dimeric complex Q8-Na-Q8 (left) side view; (right) highlight of the coordination sphere of the metal center. Hydrogen atoms have been removed for clarity

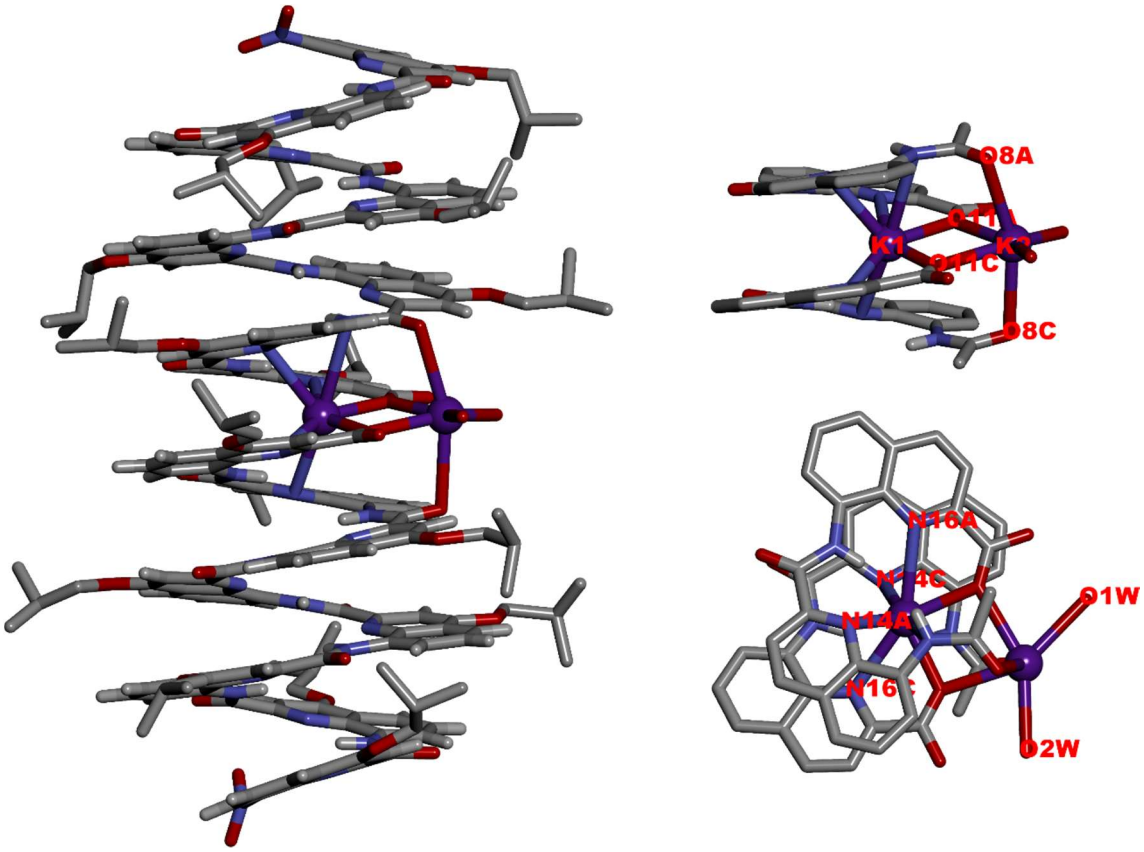

Figure S31: X-ray structures of the dimeric complex Q8-K-Q8 (left) side view; (right) highlight of the coordination sphere of the metal center. Hydrogen atoms have been removed for clarity

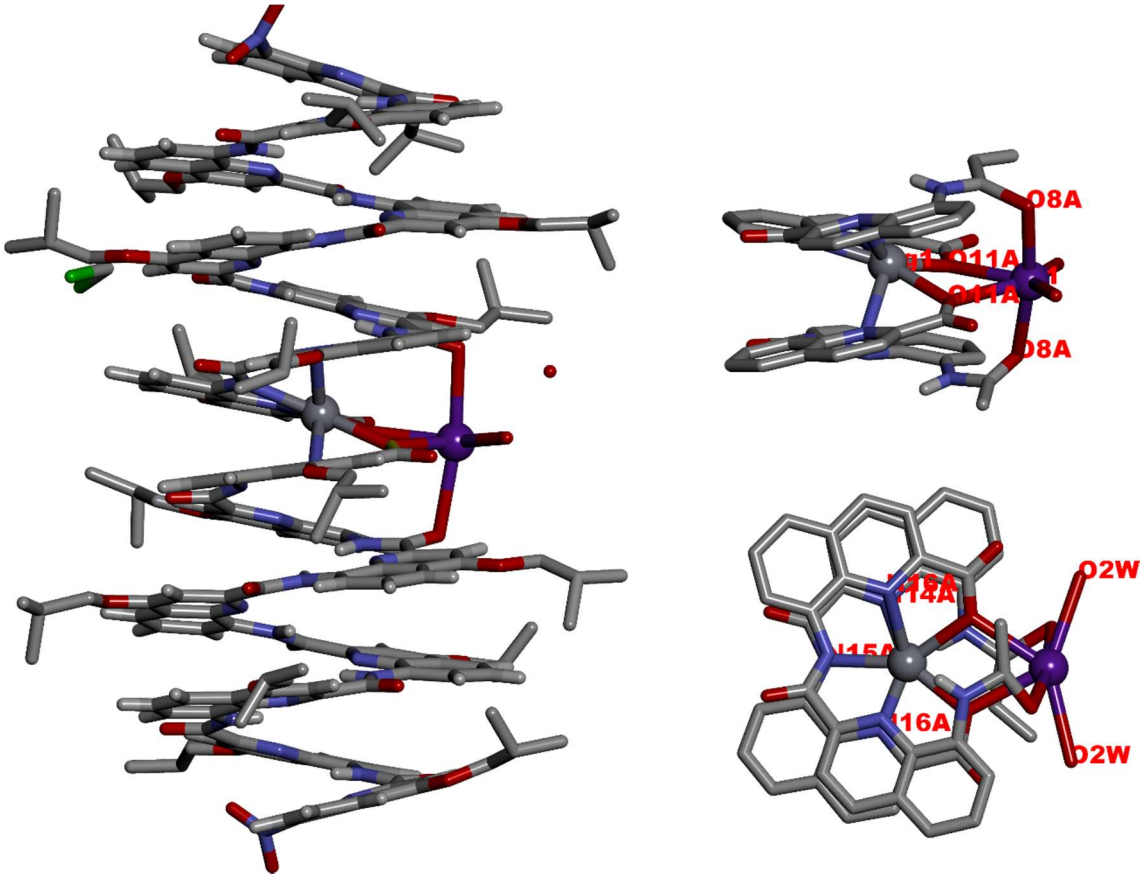

Figure S32: X-ray structures of the dimeric complex Q8-Hg-Q8 (left) side view; (right) highlight of the coordination sphere of the metal center. Mercury and potassium atoms are colored in grey and purple, respectively. Non-polar hydrogen atoms have been removed for clarity.

Table S2. Coordination spheres bond lengths (Å) in crystal structures. Atom numbers are those of the cif file.

Q_8-Na-Q_8	
Na1-O11A	2.235 (11)
Na1-O11C	2.249 (12)
Na1-N14C	2.876 (4)
Na1-N16C	2.688 (12)
Na1-N16A	2.761 (7)
Na1-N14A	3.048 (7)
Na2-O11C	2.335 (12)
Na2-O11A	2.249 (11)
Na2-O8C	2.575 (9)
Na2-O1W	2.351 (12)
Na2-O2W	2.346 (13)
Na2-Cl1	3.343 (8)
Q_8-K-Q_8	
K1-O11A	2.457 (5)
K1-O11C	2.478 (5)
K1-N14C	2.905 (5)
K1-N16C	2.863 (5)
K1-N16A	2.963 (5)
K1-N14A	2.925 (5)
K2-O11C	2.709 (6)
K2-O11A	2.755 (5)
K2-O8C	2.964 (5)
K2-O8A	2.982 (5)
K2-O1W	2.782 (10)
K2-O2W	2.777 (10)
Q_8-Hg-Q_8	
Hg1-O11A	2.337 (10)
Hg1-O11A^{i}	2.489 (10)
Hg1-N15A	2.523 (11)
Hg1-N16A	2.149 (5)
Hg1-N14A	2.666 (6)
Hg1-N16A^{i}	2.718 (5)
K2-O11A	2.764 (10)
K2-O8A	2.903 (11)
K2-O2W	2.875 (18)
K2 ion lie on a twofold axis	

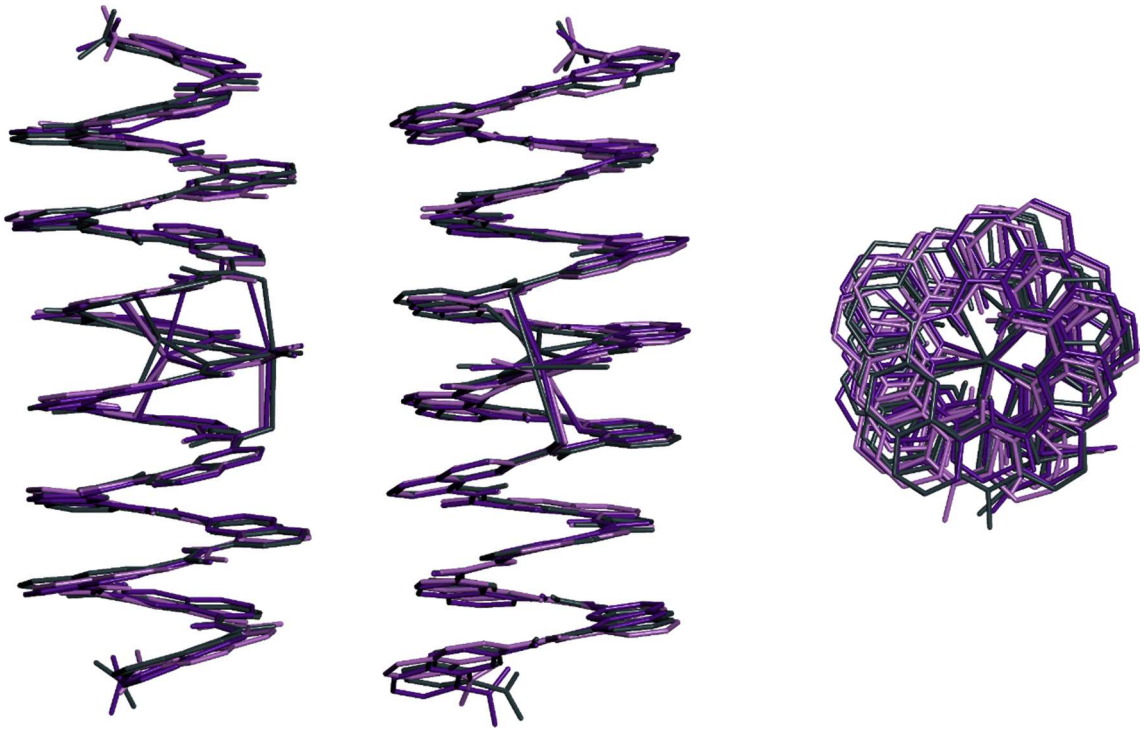

Figure S33 : Superposition of the Xray structure of Q8-Na-Q8 (light purple), Q8-K-Q8 (dark violet), Q8-Hg-Q8 (dark grey)

5. Fluroescence anisothropy decay measurements

***Preparation of the foldamer solutions*:**
Dimerization of OPV-Q_8-H was induced by adding 0.1 g of 16 M $NaOH_{(aq)}$ solution into 7 mL of OPV-Q_n-H solution in chloroform while stirring the mixture vigorously for 2 min. The heterogeneous mixture was allowed to phase separate. The foldamer solution in chloroform was withdrawn from the organic phase and placed in a fluorescence cell for absorption and fluorescence measurements.
Determination of the concentration of the foldamer species in solution: Since the deprotonated foldamers might partition between the organic and aqueous phases during the solution preparation, the foldamer concentration in chloroform was determined by UV-Vis absorption. Using the molar extinction coefficient ε_{OPV}(450 nm) for OPV in OPV-Q_8-H at 450 nm, which had been determined to equal 32,400 $M^{-1}\cdot cm^{-1}$, the concentration of OPV-Q_8CO_2H in chloroform was determined for each solution studied by applying Beer-Lambert law.[i]

***Steady-State Fluorescence (SSF)*:** All fluorescence spectra were acquired with a Horiba QM-400 spectrofluorometer equipped with a xenon arc lamp. The concentration of the OPV-Q_8-H solutions ranged between 10 nM and 1 mM covering a range of 5 orders of magnitude. Depending on whether the OPV-Q_8-H concentration was below or above 80 μM, the fluorescence spectra were acquired with the right angle or front-face geometry, respectively, with the latter geometry being used to minimize the inner filter effect.

***UV-Visible Spectrophotometer*:** The OPV-Q_8-H solutions were placed in quartz cells of path lengths equal to 0.1 mm, 1.0 mm, 1.0 cm, and 10.0 cm to ensure that an absorbance

around unity would be obtained for improved accuracy. All absorption spectra were acquired with a Cary 100 UV-Visible spectrophotometer

Time-Resolved Fluorescence Anisotropy (TRFA). The OPV-Q_8-H solutions were excited with a 479 nm delta-diode laser fitted on a HORIBA Ultima Ultrafast time-resolved fluorometer to acquire the fluorescence decays. A 480 nm bandpass filter was placed on the excitation side, and residual stray light was blocked from reaching the detector with a 495 nm cut-off filter on the emission side. All fluorescence decays were acquired up to a peak maximum of 20,000 counts. As for the SSF spectra, the right angle and front face geometries were used to acquire the fluorescence decays depending on whether the OPV-Q_8-H concentration was below or above 80 μM, respectively. The instrument response function was collected by reflecting the nano-LED light from a triangular aluminum monolith without the 495 nm cut-off filter. A time-per-channel (TPC) of 1.28×10^{-2} ns/channel across 4,096 channels was used for all decay acquisitions. For each TRFA experiment, three fluorescence decays, namely $I_{VM}(t)$, $I_{VV}(t)$, and $I_{VH}(t)$, were acquired using vertically polarized excitation light and the polarization of the emission set at the magic angle, the vertical and horizontal direction with respect to the polarization of the excitation light, respectively.

***TRFA decay analysis*:** The $I_{VV}(t)$ and $I_{VH}(t)$ fluorescence decays were analyzed globally with the programs aniso01d-4k and aniso01d-7k using a single rotational time. The former program optimized the OPV lifetime (τ_o) obtained at the magic angle, and the latter used a fixed τ_o value. The parameters obtained with the program yielding a better χ^2 were selected for the plot shown in Figure 4 in the main text. The $I_M(t)$ decay of the OPV-Q_8-H solution was fitted with a monoexponential function, as shown in Equation 1, to determine the lifetime τ_o of the OPV label covalently attached to the foldamer. τ_o was found to equal 1.60 (±0.01) ns, which is typical of this compound.[i,ii]

$$I_{VM}(t) = I_o \exp(-t/\tau_o) \quad (1)$$

In Equation 1, I_o is the initial fluorescence intensity and t is the time in nanoseconds. The $I_{VV}(t)$ and $I_{VH}(t)$ decays were then fitted globally according to Equations 2 and 3, respectively.

$$I_{VV}(t) = \frac{I_o}{3}\exp(-t/\tau_o)\times[1+2r(t)] \quad (2)$$

$$I_{VH}(t) = \frac{I_o}{3G}\exp(-t/\tau_o)\times[1-r(t)] \quad (3)$$

The G-factor being a scaling constant, was optimized during the analysis. Contrary to the traditional methodology involving the separate experimental determination of the G-factor, including the G-factor in the optimization of the parameters describing $r(t)$ in Equations 2 – 4 has been found to be a methodology that is much more straightforward, accurate, rapid, and reliable.[i,ii] $r(t)$ can be approximated by a sum of 3 exponentials for

symmetric top macromolecules, such as OPV-Q_8-H and its dimer, as shown in Equation 4.[iii]

$$r(t) = r_o \sum_{i=1}^{n} a_i \exp(-t / \phi_i) \quad (4)$$

In Equation 4, r_o is the anisotropy at time t equal zero. Global analysis of the polarized fluorescence decays $I_{VV}(t)$, and $I_{VH}(t)$ using a single exponential in Equation 4 yielded the average rotational time $<\phi>$ corresponding to a mixture of OPV-Q_8-H and its dimer. The parameters of the fit were optimized according to the Marquardt-Levenberg algorithm.

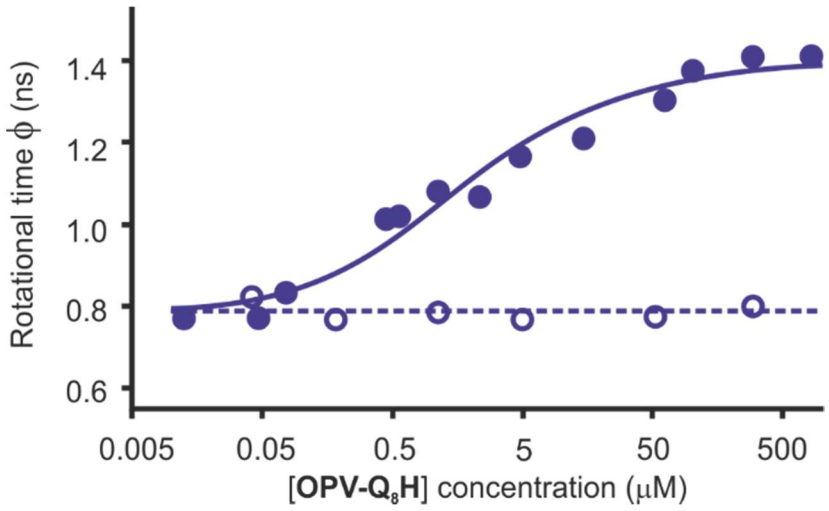

Figure S34: Plot of the average rotational time $<\phi>$ as a function of OPV-Q8H concentration in chloroform (○) without and (●) in presence of a 16 M NaOH aqueous solution.

6. Preparation of longer metal complexes: insertion experiments by NMR and CD

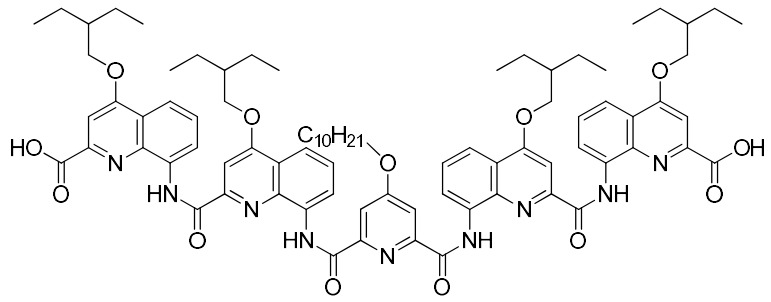

H-Q_2PQ_2-H

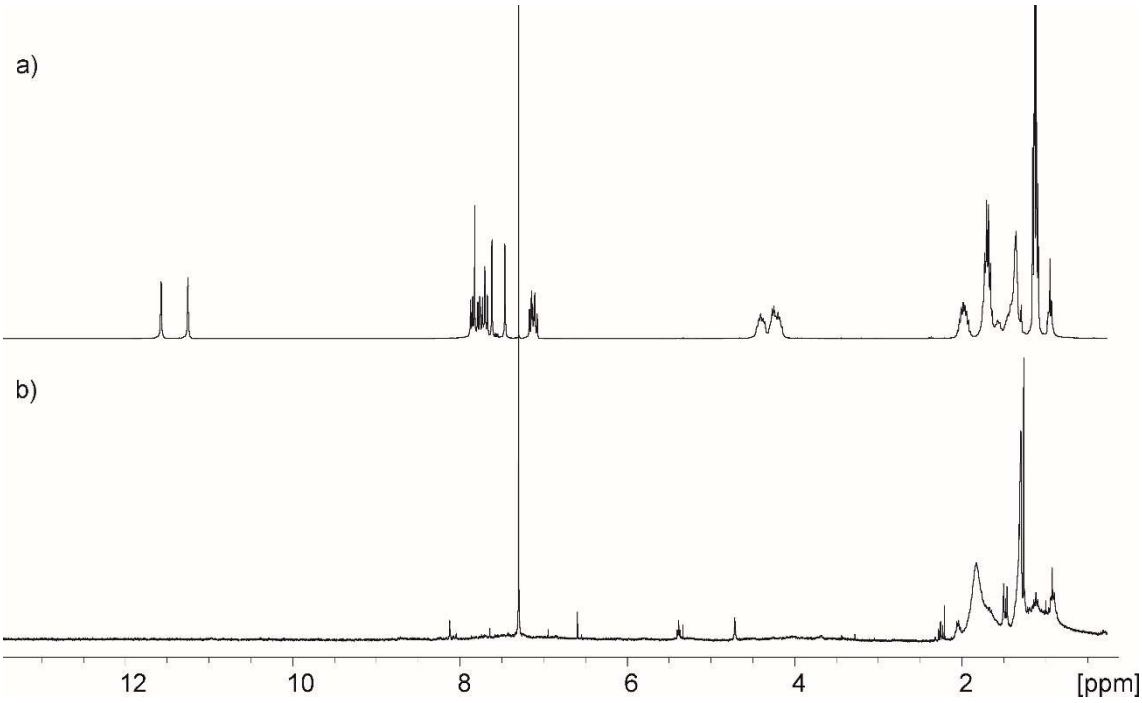

Figure S35. ^{1}H NMR spectra of a $CDCl_3$ solution of a) H-Q_2PQ_2-H and b) CO_2H-Q_2PQ_2-CO_2H in the presence of sodium hydroxide excess

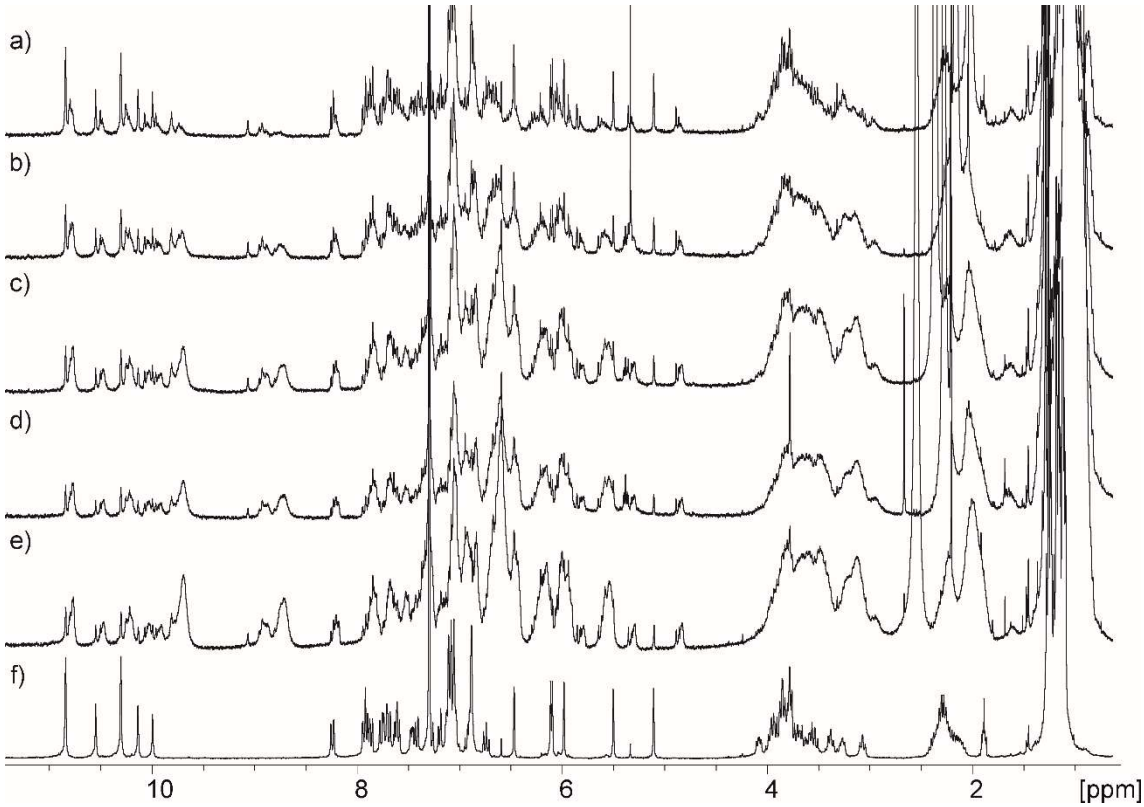

Figure S36. ^{1}H NMR titration (300 MHz, 298K) of a $CDCl_3$ solution of Q_8-Na-Q_8 with increasing amounts of HQ_2PQ_2H in the presence of NaOH excess a) 0.5 equiv. b) 1 equiv. c) 1.5 equiv. d) 2 equiv. e) 3 equiv. f) 0 equiv.

CD samples preparation: Samples were prepared independently by mixing *R*-Q_8H with the corresponding amount of H-Q_2PQ_2-H in dry $CHCl_3$. Then, each sample was incubated with silver acetate excess in the dark for 24h before measurement to ensure the complete formation of the complexes (kinetic stabilization). The initial concentration of R-Q8-H = 1 mM. A cuvettes with an optical path of 0.1 mm was used for measurements.

7. Experimental procedures

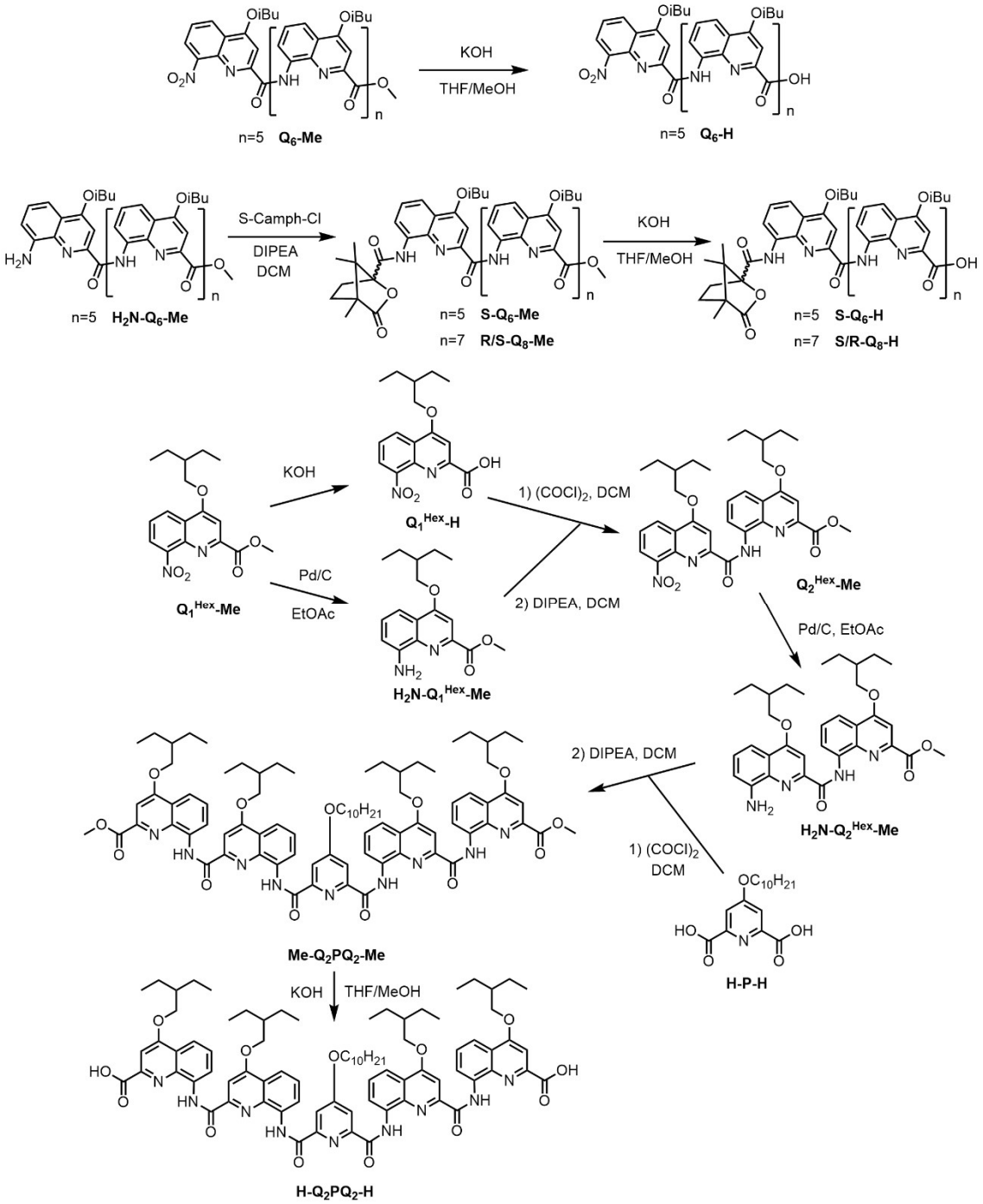

Synthesis of Q_6-H

In a 25mL round-bottom flask, **Q6-Me** [iv] (225 mg, 0.15 mmol) is dissolved in 10 mL of THF and 2 mL of methanol. Then, finely ground KOH (42 mg, 0.75 mmol) is added in one portion. The reaction is stirred overnight at room temperature. Citric acid 5% solution is added until pH ca. 5. Then the THF is removed under reduced pressure. The residue is extracted with dichloromethane (15 mL) and washed with water (15 mL) and brine (15 mL). The organic layer is dried with magnesium sulfate, and the solvent is evaporated to afford Q_6-H as a yellow solid (150 mg, 76% yield).

^{1}H NMR ($CDCl_3$, 300 MHz): δ (ppm) 11.64 (s, 1H), 11.60 (s, 1H), 11.41 (s, 1H), 11.40 (s, 1H), 11.11 (s, 1H), 8.58 (dd, 1H), 8.44 (dd, 1H), 8.40 (dd, 1H), 8.34 (dd, 1H), 8.20 (dd, 1H), 8.14 (dd, 1H), 8.11 (dd, 1H), 8.08 (dd, 1H), 8.05 (dd, 1H), 7.92 (dd, 1H), 7.70 (t, 1H), 7.57-7.34 (m, 7H), 7.21 (t, 1H), 7.20 (s, 1H), 7.00 (s, 1H), 6.86 (s, 1H), 6.62 (s, 1H), 6.52 (s, 1H), 4.42 (dd, 1H), 4.26-3.83 (m, 11H), 2.62-2.23 (m, 6H), 1.37-1.16 (m, 36H).

^{13}C NMR ($CDCl_3$): δ (ppm) 163.5, 163.2, 163.0, 162.9, 162.6, 161.1, 160.9, 160.6, 160.1, 159. 9, 153.0, 150.3, 150.1, 148.5, 148.3, 144.9, 140.4, 138.8, 138.3, 138.0, 137.9, 137.5, 137.3, 134.1, 133.6, 133.3, 132.9, 132.4, 127.9, 127.5, 127.1, 127.0, 126.6, 125.9, 125.5, 124.0, 123.6, 122.5, 122.3, 122.2, 121.9, 121.8, 117.6, 117.2, 116.9, 116.8, 116.5, 116.4, 115.9, 115.7, 99.6, 98.7, 98.5, 97.9, 97.8, 75.6, 75.5, 75.4, 75.3, 75.2. 29.5, 28.3, 28.2, 28.1, 28.0, 27.9, 19.5, 19.4, 19.3, 19.2, 19.1

HRMS (ES^+): m/z calc for $C_{84}H_{85}N_{12}O_{15}$ 1501.62573 $[M+H]^+$ found 1501.63041

Synthesis of R-Q_8-H or S-Q_8-H

In a 25 mL round-bottom flask, **H_2N-Q_8-Me** [v](309 mg, 0.20 mmol) is dissolved in 10 mL of dry dichloromethane. Under a nitrogen atmosphere, 0.1 mL of dry diisopropylamine is added. Then at 0ºC, (*R*)-camphanyl chloride (for R-Q8-H) or (*S*)-camphanyl chloride(for S-Q8-H) (65 mg, 0.3 mmol) dissolved in 5 mL of dry dichloromethane is added dropwise. The flask is stirred for 2h. Then, the reaction is washed (2x10 mL) with water, saturated aqueous $NaHCO_3$, citric acid 10% and brine. The organic layer is dried with magnesium sulfate and concentrated under reduced pressure. The crude is dissolved directly in 10 mL of THF and 2 mL of methanol in the presence of KOH powder (80 mg, 1.42 mmol) for 18h at room temperature. Citric acid 5% solution is added until pH reaches ca. 5. Then the THF is removed under reduced pressure. The residue is extracted with dichloromethane (10 mL) and washed with water (10 mL) and brine (10 mL). The organic layer is dried with magnesium sulfate and dried under vacuum to afford after column chromatography **R-Q_8-H** or **S-Q_8-H** as a yellow solid (280 mg, 95%).

^{1}H NMR ($CDCl_3$, 300 MHz): δ (ppm) 11.39 (s, 1H), 11.35 (s, 1H), 11.24 (s, 1H), 11.03 (s, 1H), 10.97 (s, 1H), 10.89 (s, 1H), 10.88 (s, 1H), 9.43 (s, 1H), 8.24 (dd, 2H), 8.19 (dd, 1H), 8.15 (dd, 1H), 8.06 (dd, 1H), 7.94 (dd, 1H), 7.94-7.78 (m, 8H), 7.68 (dd, 1H), 7.52-7.31 (m, 5H), 7.24 (m, 2H), 7.04 (m, 2H), 6.96 (s, 1H), 6.90 (s, 1H), 6.86 (s, 1H), 6.72 (s, 1H), 6.55 (s, 1H), 6.52 (s, 1H), 6.48 (s, 1H), 6.10 (s, 1H), 4.21-3.66 (m, 16H), 2,60-2.30 (m, 8H), 1,43-1,11 (m, 52H), 1.06 (s, 3H), 0.61 (s, 3H), 0.59 (s, 3H)

^{13}C NMR ($CDCl_3$): δ (ppm) 178.3, 175.6, 164.4, 163.1, 162.9, 162.8, 162.7, 162.6, 162.5, 162.2, 162.1, 162.0, 160.7, 160.6, 160.3, 159.2, 159.0, 158.9, 150.0, 149.6, 149.5, 148.7, 148.6, 148.2, 148.1, 144.0, 137.7, 137.6, 137.4, 137.2, 137.1, 137.0, 136.9, 133.2, 133.1, 132.9, 132.8, 132.7, 132.6, 132.2, 132.1, 127.5, 127.0, 126.3, 126.1, 126.0, 125.9, 125.8, 127.6, 122.3, 122.2, 122.1, 122.0, 121.9, 121.8, 121.7, 121.5. 117.6, 117.3, 117.1, 116.6, 116.5, 116.2, 116.0, 115.8, 115.6, 116.0, 115.8, 115.6, 115.5, 99.4, 98.9, 98.6, 98.4, 98.3, 97.7, 91.4, 75.3, 75.2-74.9, 55.0, 54.3, 54.1, 53.9, 30.7, 29.7, 29.4, 29.1, 28.6, 28.4, 28.2, 28.1, 28.0, 27.9, 19.7-19.1, 16.8, 16.7, 16.1, 15.8, 14.1, 9.8, 9.4

HRMS (ES^+): m/z calc for $C_{122}H_{127}N_{16}O_{20}$ 2135.94126 $[M+H]^+$ found 2135.94091

Synthesis of S-Q$_6$-H

In a 25 mL round-bottom flask, **H2N-Q6-Me** [iv] (95 mg, 64 μmol) is dissolved in 5 mL of dry dichloromethane. Under a nitrogen atmosphere, 0.1 mL of dry diisopropylamine is added. Then at 0ºC, (*S*)-camphanyl chloride (21 mg, 97 μmol) dissolved in 2 mL of dry dichloromethane is added dropwise. The flask is stirred overnight at room temperature. The reaction is washed (2x10 mL) with water, sat $NaHCO_3$, citric acid 10% and brine. The organic layer is dried with magnesium sulfate and concentrated under reduced pressure. The crude is dissolved directly in 10 mL of THF and 2 mL of methanol in the presence of KOH powder (30 mg, 0.53 mmol) for 18h. Citric acid 5% solution is added until pH ca. 5. Then the THF is removed under reduced pressure. The residue is extracted with dichloromethane (10 mL) and washed with water (10 mL) and brine (10 mL). The organic layer is dried with magnesium sulfate and evaporated to afford after flash chromatography, **S-Q$_6$-H** as a yellow solid (87 mg, 86%).

^{1}H NMR ($CDCl_3$, 300 MHz): δ (ppm) 11.80 (s, 1H), 11.64 (s, 1H), 11.52 (s, 1H), 11.33 (s, 1H), 11.11 (s, 1H), 9.65 (s, 1H), 8.69 (dd, 1H), 8.33 (dd, 1H), 8.14 (dd, 2H), 8.07-7.96 (m, 5H), 7.93 (dd, 1H), 7.85 (dd, 1H), 7.80 (dd, 1H), 7.75-7.64 (m, 2H), 7.52 (t, 1H), 7.37-7.31 (m, 3H), 7.16 (t, 1H), 7.10 (s, 1H), 6.99 (s, 1H), 6.82 (s, 1H), 6.63 (s, 1H), 6.40 (s, 1H), 4.45-3.86 (m, 12H), 2.62-2.26 (m, 6H), 1.41-1.17 (m, 40H), 0.69 (t, 3H), 0.67 (t, 3H), 0.23 (t, 3H)

^{13}C NMR ($CDCl_3$): δ (ppm) 176.2, 164.6, 163.4, 163.2, 163.1, 162.9, 162.7, 162.3, 160.9, 160.8, 160.4, 158.9, 150.2, 150.0, 149.8, 148.6, 148.5, 143.3, 138.0, 137.9, 137.4, 137.1, 133.5, 133.2, 132.8, 132.6, 132.4, 127.6, 127.0, 126.4, 126.2, 126.1, 125.7, 122.4, 121.8, 121.7, 117.6, 117.5, 116.8, 116.7, 116.6, 116.4, 116.0, 115,6, 115.4, 99.7, 99.4, 98.5, 98.4, 98.3, 97.8, 91.6, 75.3, 75.2, 75.1, 55.4, 55.0, 29.7, 29.4, 28.4, 28.2, 28.1, 28.0, 19.6, 19.4, 19.3, 19.2, 16.1, 15.9, 9.5

HRMS (ES^+): m/z calc for $C_{94}H_{99}N_{12}O_{16}$ 1651.73020 $[M+H]^+$ found 1651.73487

Synthesis of H$_2$N-Q$_1^{Hex}$-Me

In a 100 mL round-bottomed flask, **Q$_1^{Hex}$-Me** (1.9 g, 5.7 mmol) was dissolved in 40 mL of ethyl acetate. Palladium on carbon (10%, 190 mg) was added in one portion, and the flask was stirred under a hydrogen atmosphere for four hours until completion. Then the reaction is filtered over Celite and concentrated under reduced pressure without further purification to afford 1.8g (99%) of **H$_2$N-Q$_1^{Hex}$-Me** as a yellow solid.

^{1}H NMR ($CDCl_3$, 300 MHz): δ (ppm) 7.54 (s, 1H), 7.53 (dd, 1H), 7.40 (t, 1H), 6.97 (dd, 1H), 4.18 (d, 2H), 4.06 (s, 3H), 1.88 (m, 1H), 1.62 (m, 4H), 1.02 (t, 6H)

^{13}C NMR ($CDCl_3$): δ (ppm) 166.7, 162.8, 145.9, 144.9, 138.4, 128.6, 123.1, 110.9, 109.6, 100.8, 70.8, 52.9, 40.9, 25.6, 11.2

HRMS (ES^+): m/z calc for $C_{17}H_{23}N_2O_3$ $[M+H]^+$ 303.17089 found 303.17027

Synthesis of Q_2^{Hex}-Me

In a 50 mL round-bottomed flask, **Q_1^{Hex}-H** (2.17g, 6.8 mmol) was dissolved in 20 mL of dry dichloromethane and stirred for an hour in the presence of oxalyl chloride (0.86 mL, 1.5 eq) under a nitrogen atmosphere to form the acid chloride. Then, it is dried under a high vacuum for at least three hours.

In a 100 mL round-bottomed flask, **H_2N-Q_1^{Hex}-Me** (1.6 g, 5.3 mmol) was dissolved in 20 mL of dry dichloromethane in the presence of 3 eq of dry diisopropylamine. Under a nitrogen atmosphere, the previously prepared acid chloride is added dropwise at 0ºC as a solution in 10 mL of dry dichloromethane. The reaction is stirred for an hour, then is concentrated under reduced pressure, triturated in hexanes and filtered to afford **Q_2^{Hex}-Me** as a dark yellow solid (2.9g, 91%) without further purification required.

^{1}H NMR ($CDCl_3$, 300 MHz): δ 11.92 (s, 1H), 9.12 (dd, 1H), 8.53 (dd, 1H), 8.23 (dd, 1H), 8.02 (dd, 1H), 8.01 (s, 1H), 7.68 (m, 3H), 4.33 (d, 2H), 4.24 (s, 3H), 4.23 (d, 2H), 1.92 (m, 4H), 1.64 (m, 8H), 1.03 (12H)

^{13}C NMR ($CDCl_3$): δ (ppm) 167.0, 163.4, 162.9, 162.6, 154.0, 148.4, 147.9, 139.8, 139.4, 134.9, 127.9, 126.7, 125.4, 123.5, 122.4, 118.8, 116.8, 101.5, 100.2, 71.8, 71.1, 53.7, 53.6, 41.9, 40.8, 40.7, 23.6, 23.5, 11.2, 11.1

HRMS (ES^+): m/z calc for $C_{33}H_{39}N_4O_7$ $[M+H]^+$ 603.28187 found 603.28142

Synthesis of H_2N-Q_2^{Hex}-Me

In a 100 mL round-bottom flask, **Q_2^{Hex}-Me** (300 mg, 0.5 mmol) was dissolved in 15 mL of ethyl acetate. Palladium on carbon (10%, 30 mg) was added in one portion, and the flask was stirred under a hydrogen atmosphere overnight until completion. Then the reaction is filtered over Celite and concentrated under reduced pressure without further purification to afford 290 mg (99%) of the amine as a yellow solid which was used without further purification.

^{1}H NMR ($CDCl_3$, 300 MHz): δ 12.78 (s, 1H), 9.10 (dd, 1H), 7.97 (dd, 1H), 7.82 (s, 1H), 7.70 (t, 1H), 7.62 (s, 1H), 7.57 (dd, 1H), 7.42 (t, 1H), 7.05 (dd, 1H), 4.28 (d, 2H), 4.25 (d, 2H), 4.15 (s, 3H), 1.91 (m, 4H), 1.64 (m, 8H), 1.05 (12H)

^{13}C NMR ($CDCl_3$): δ (ppm) 165.3, 163.3, 163.1, 163.0, 148.2, 146.7, 144.8, 139.5, 137.3, 135.2, 128.4, 128.1, 123.0, 122.2, 117.1, 115.6, 110.9, 109.5, 101.3, 98.2, 71.1, 70.9, 52.9, 40.9, 23.6, 23.5, 11.3

HRMS (ES$^+$): m/z calc for $C_{33}H_{41}N_4O_5$ $[M+H]^+$ 573.30770 found 573.30755

Synthesis of Me-Q_2PQ_2-Me

In a 25 mL round-bottom flask **H-P-H** [vi] (73 mg, 0.23 mmol) is dissolved in 1 mL of dry dichloromethane. Oxalyl chloride (0.2 mL) is added dropwise at 0 ºC under a nitrogen atmosphere. The reaction is stirred for one hour at room temperature until the complete formation of the acid chloride is confirmed by NMR. Solvent and excess oxalyl chloride are then evaporated under vacuum, and the solid diacid chloride is then redissolved in 5mL of dry dichloromethane to be used in the subsequent reaction.

In a 50 mL round-bottom flask **H_2N-Q_2^{Hex}-Me** (290 mg, 0.5 mmol) is dissolved in 10 mL of dry dichloromethane in the presence of 0.2 mL of dry diisopropylamine. Under a nitrogen atmosphere, the previously prepared diacid chloride solution is then added dropwise. The reaction is stirred for 2 h, then is concentrated under reduced pressure, filtered on a short pad of silica gel eluting with dichloromethane: ethyl acetate 9:1 and further purified by GPC to obtain 210 mg (63%) of a bright yellow solid.

^{1}H NMR ($CDCl_3$, 300 MHz): δ 11.85 (s, 2H), 11.66 (s, 2H), 8.08 (dd, 2H), 7.85 (s, 2H), 7.84 (d, 2H), 7.73 (s, 2H), 7.72 (dd, 2H), 7.60 (dd, 2H), 7.41 (s, 2H), 7.23 (t, 2H), 7.04 (t, 2H), 4.53-4.13 (m, 10H), 3.28 (m, 6H), 2.00 (m, 4H), 1.69 (m, 16H), 1.18-1.04 (m, 20H), 0.95 (t, 3H)

^{13}C NMR ($CDCl_3$): δ (ppm) 167.8, 164.9, 163.4, 162.8, 162.2, 161.3, 151.7, 150.2, 146.2, 138.9, 138.3, 133.8, 133.5, 127.9, 127.5, 122.0, 121.7, 116.8, 116.2, 116.1, 115.5, 111.4, 101.6, 99.5, 75.4, 71.5, 71.1, 52.2, 40.9, 40.8, 28.1, 23.7, 19.2, 11.3, 11.2

HRMS (ES$^+$): m/z calc for $C_{83}H_{102}N_9O_{13}$ $[M+H]^+$ 1432.75971 found 1432.76130

Synthesis of H-Q_2PQ_2-H

In a 100 mL round-bottom flask, **Me-Q_2PQ_2-Me** (50 mg, 35 μmol) is dissolved in 10 mL of THF and 1 mL of methanol. Then, finely ground KOH (30 mg, 0.5 mmol) is added. The reaction is stirred overnight at room temperature. The reaction was acidified with 5% citric acid solution and was extracted with dichloromethane. The combined organic layers were washed with water and brine, dried over magnesium sulfate and concentrated under reduced pressure to afford 43 mg (88%) of a bright pale yellow solid.

^{1}H NMR ($CDCl_3$, 300 MHz): δ 11.57 (s, 2H), 11.25 (s, 2H), 7.85 (dd, 2H), 7.82 (s, 2H), 7.77 (d, 2H), 7.70 (s, 2H), 7.70 (dd, 2H), 7.61 (s, 2H), 7.46 (s, 2H), 7.18-7.06 (m, 4H), 4.47-4.13 (m, 10H), 1.98 (m, 4H), 1.70 (m, 16H), 1.16-1.02 (m, 20H), 0.95 (t, 3H)

^{13}C NMR ($CDCl_3$): δ (ppm) 168.7, 164.0, 163.6, 163.3, 161.7, 160.9, 151.2, 149.7, 145.2, 138.0, 137.4, 133.1, 132.7, 128.3, 127.8, 122.3, 121.9, 117.0, 116.7, 116.0, 115.9, 112.3, 99.9, 99.4, 71.8, 71.6, 69.4, 40.7, 32.0, 29.6, 29.5, 29.4, 28.9, 25.9, 23.6, 22.7, 14.2, 11.3

HRMS (ES$^+$): m/z calc for $C_{81}H_{98}N_9O_{13}$ $[M+H]^+$ 1404.72841 found 1404.73122

^{1}H NMR and ^{13}C NMR spectra of new synthetic compounds

Q_6-H

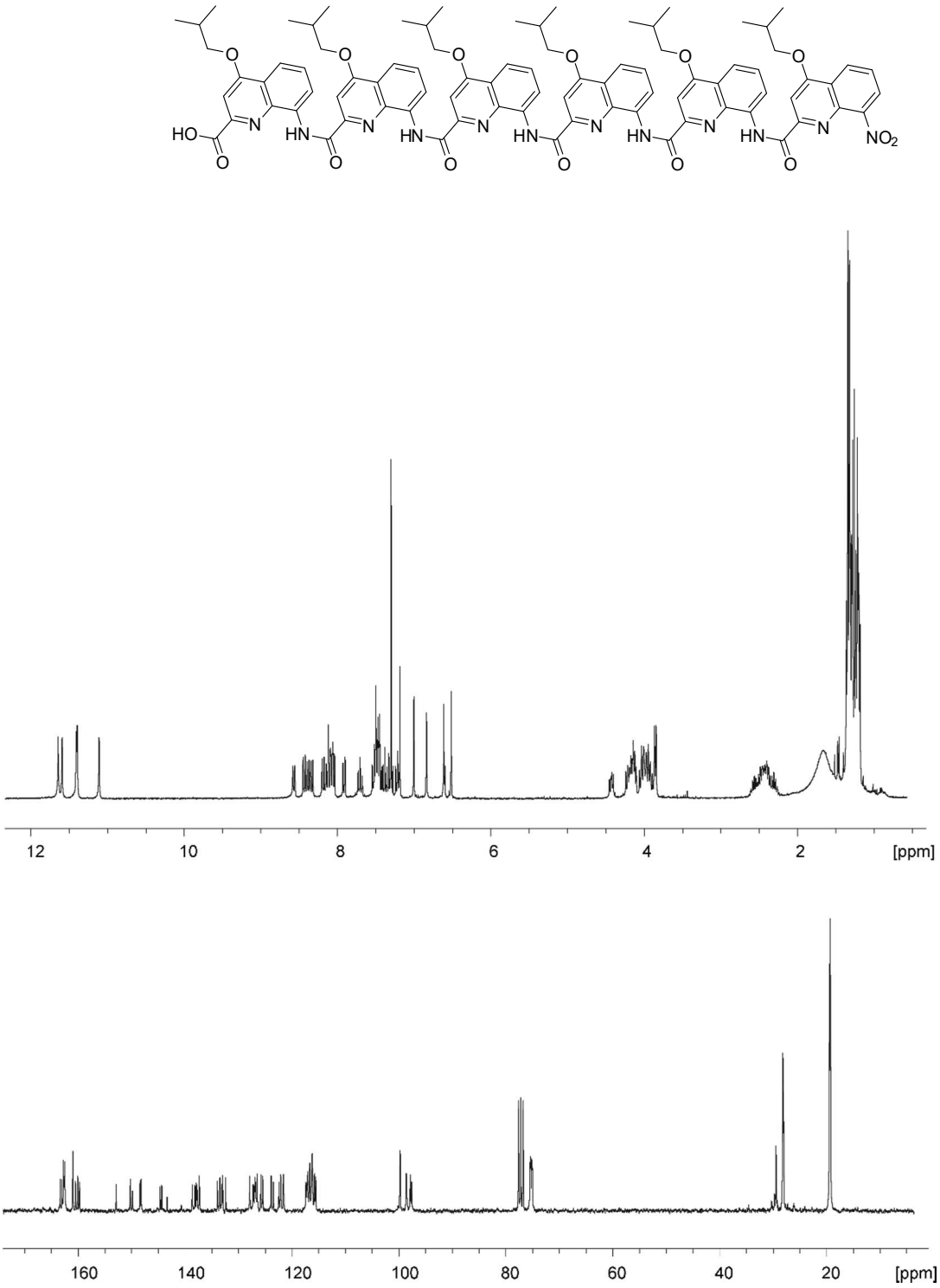

Figure S37. ^{1}H and ^{13}C NMR spectra of a $CDCl_3$ solution of **Q_6-H**

R-Q_8-H or S-Q8-H : similar NMR

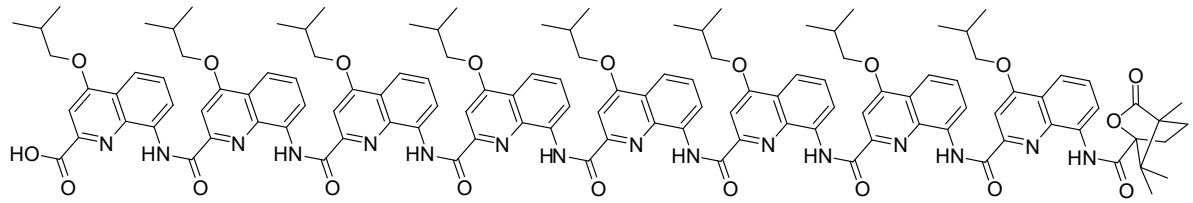

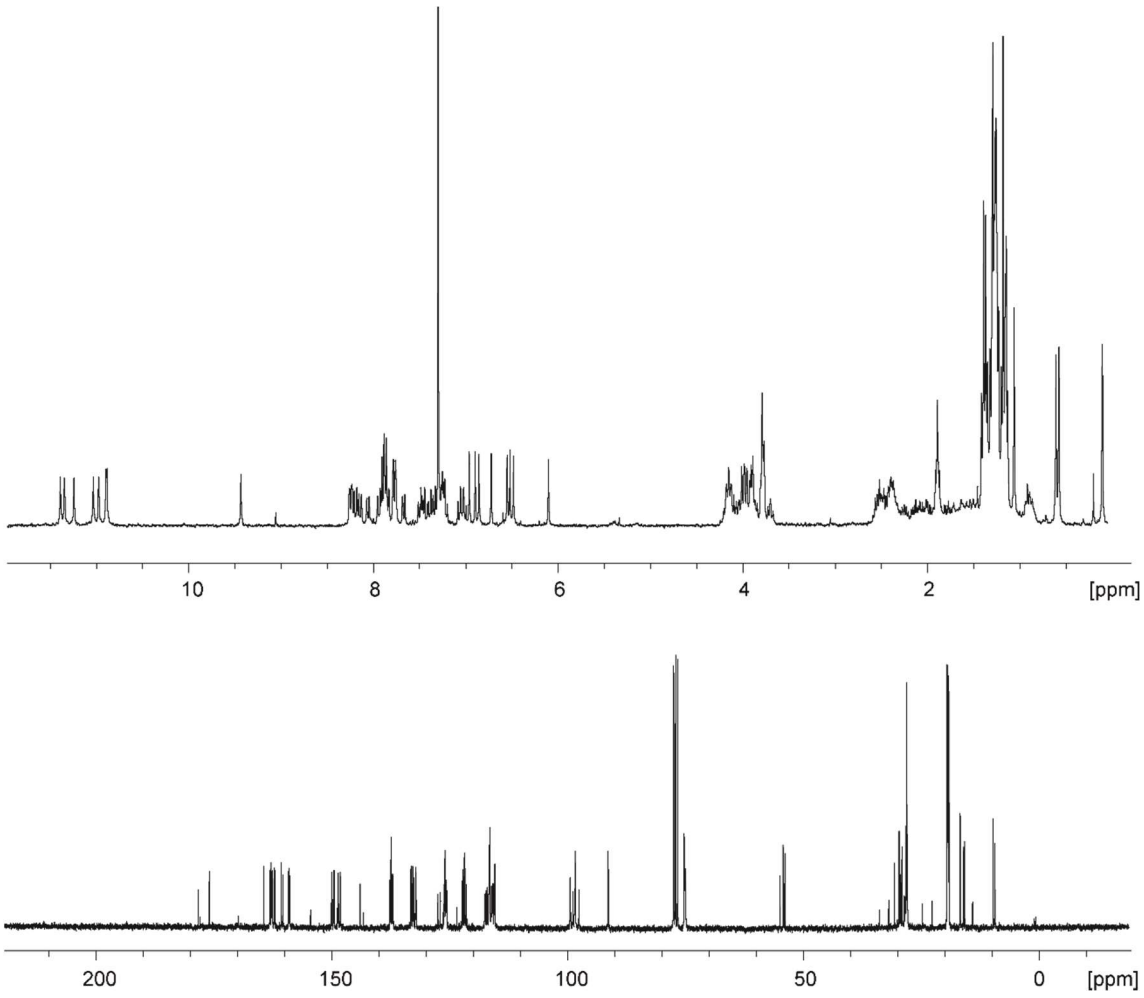

Figure S38. ^{1}H and ^{13}C NMR spectra of a $CDCl_3$ solution of **R-Q8-H or S-Q8-H**

S-Q$_6$-H

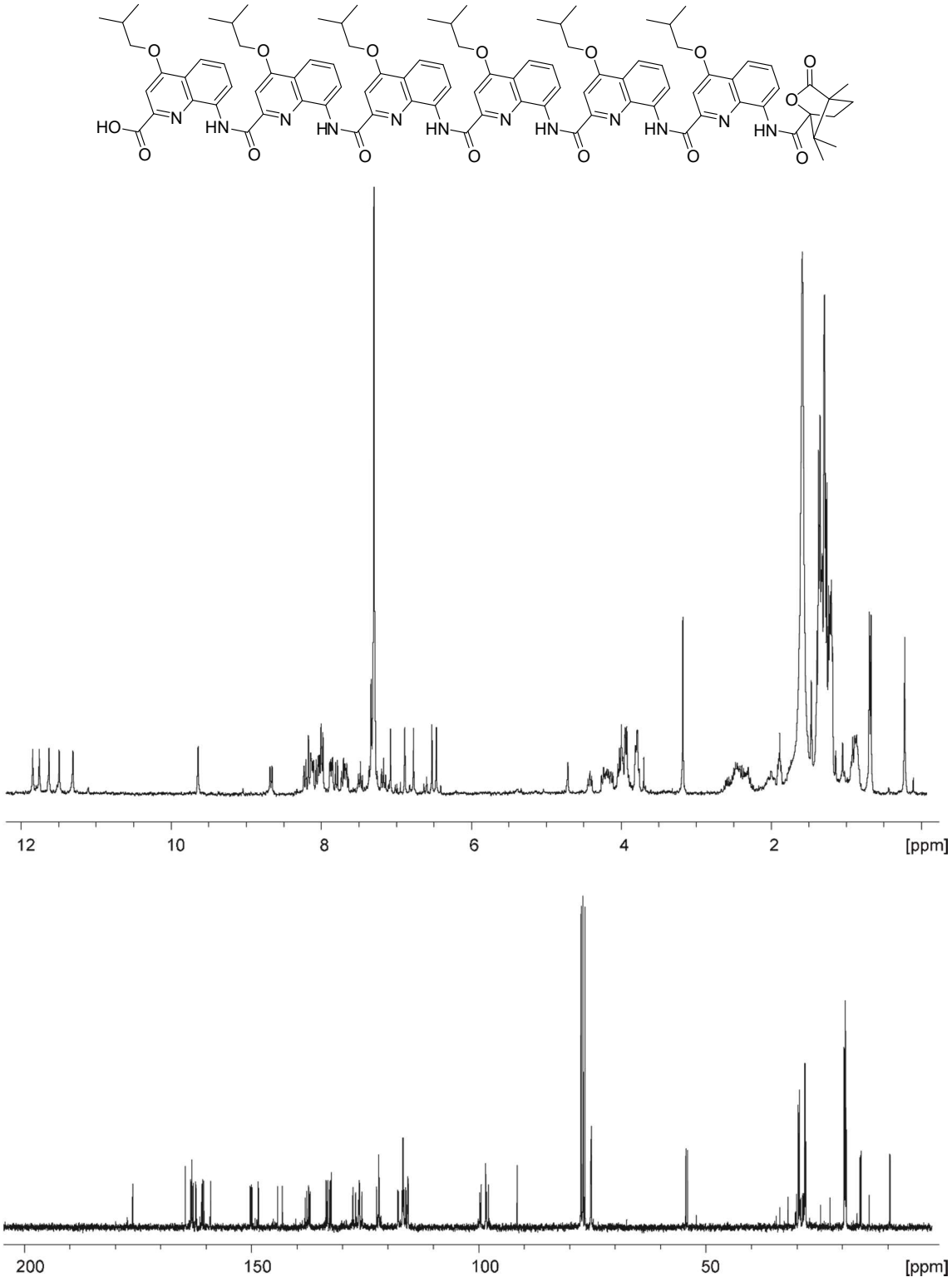

Figure S39. ^{1}H and ^{13}C NMR spectra of a $CDCl_3$ solution of **S-Q$_6$-H**

H_2N-Q_1^{Hex}-Me

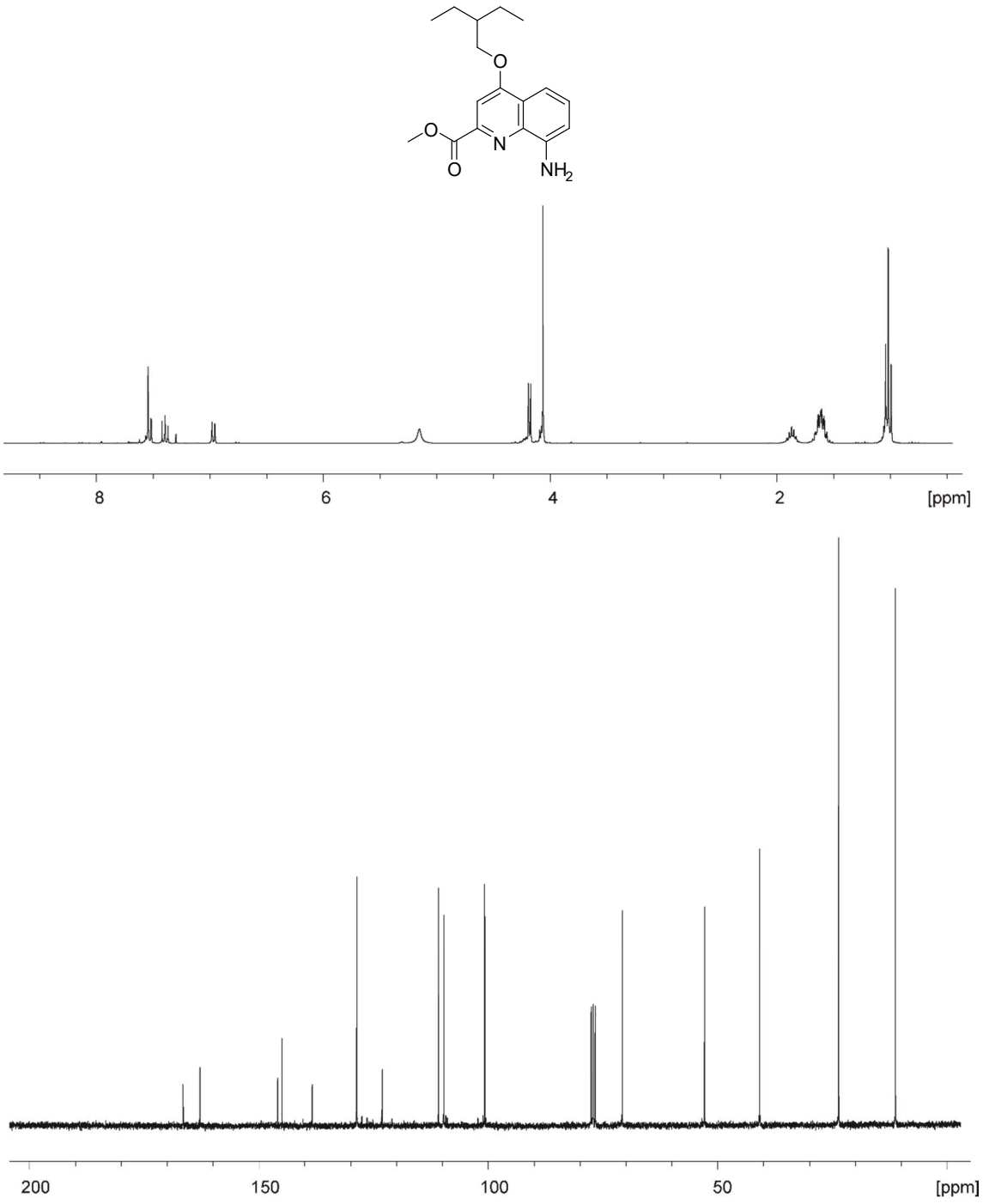

Figure S40. ^{1}H and ^{13}C NMR spectra of a $CDCl_3$ solution of **H_2N-Q_1^{Hex}-Me**

<u>Q_2^{Hex}-Me</u>

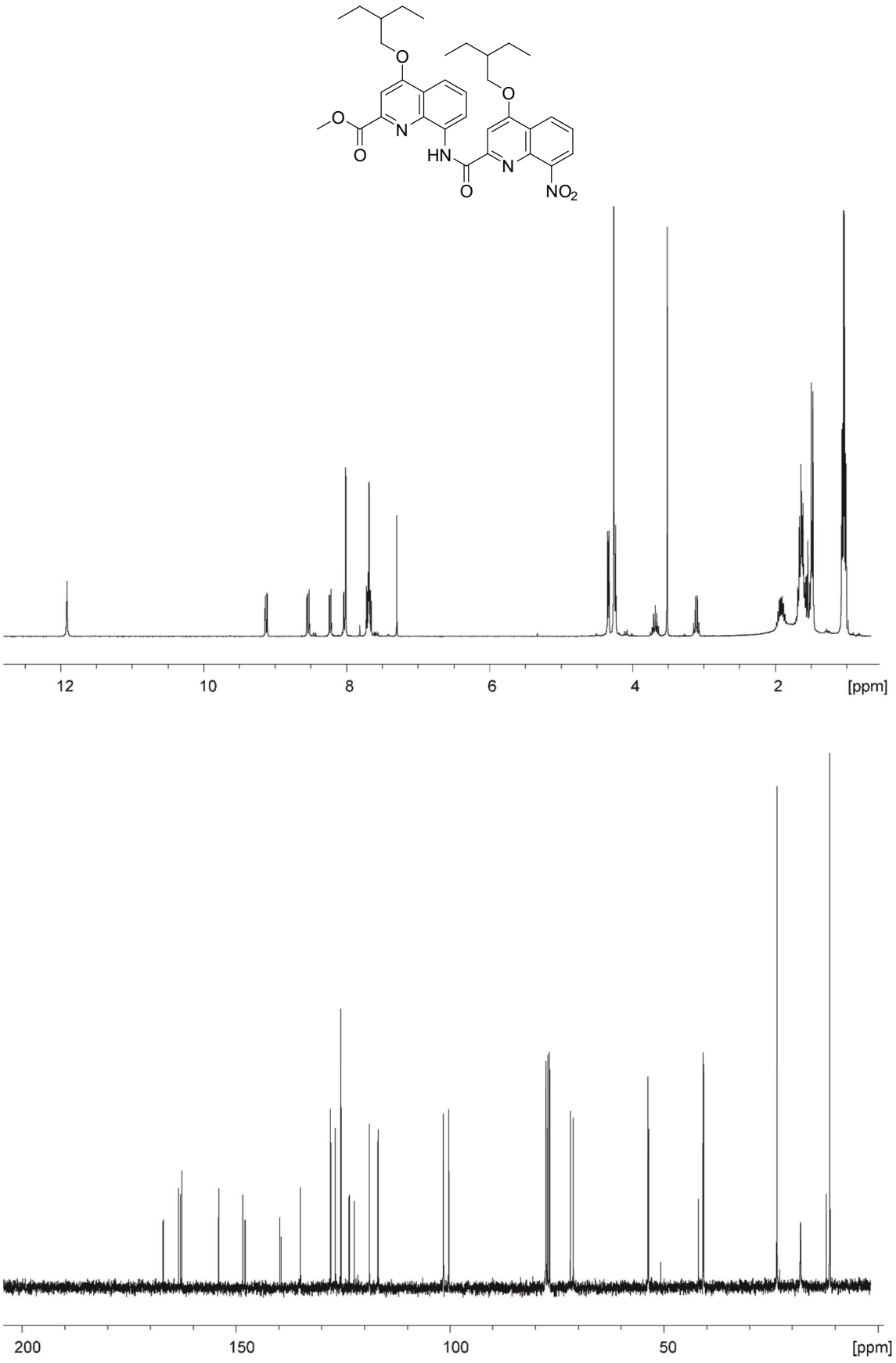

Figure S41. ^{1}H and ^{13}C NMR spectra of a $CDCl_3$ solution of **Q_2^{Hex}-Me**

H₂N-Q₂^{Hex}-Me

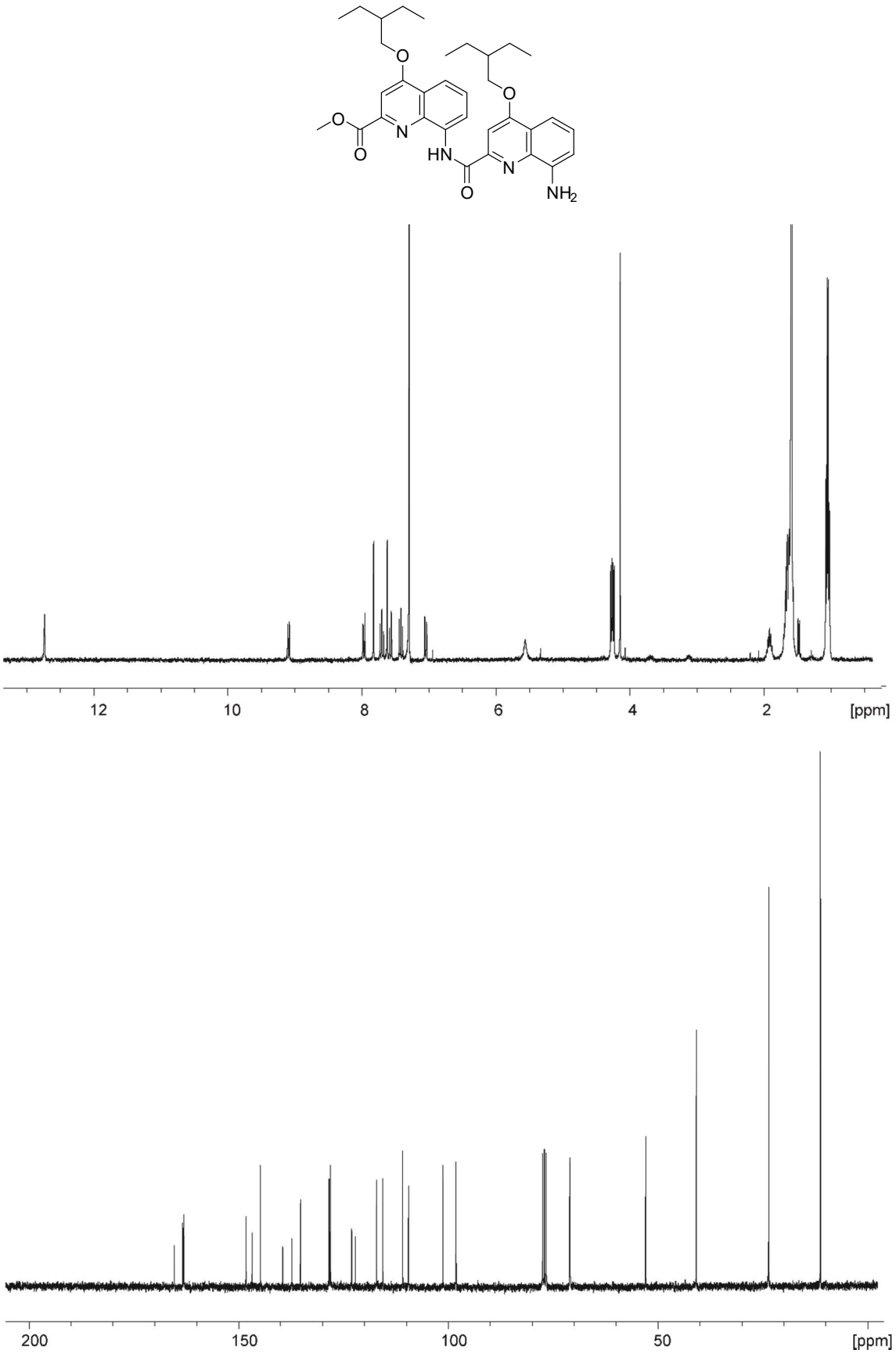

Figure S42. ^{1}H and ^{13}C NMR spectra of a $CDCl_3$ solution of **H_2N-Q_2^{Hex}-Me**

Me-Q_2PQ_2-Me

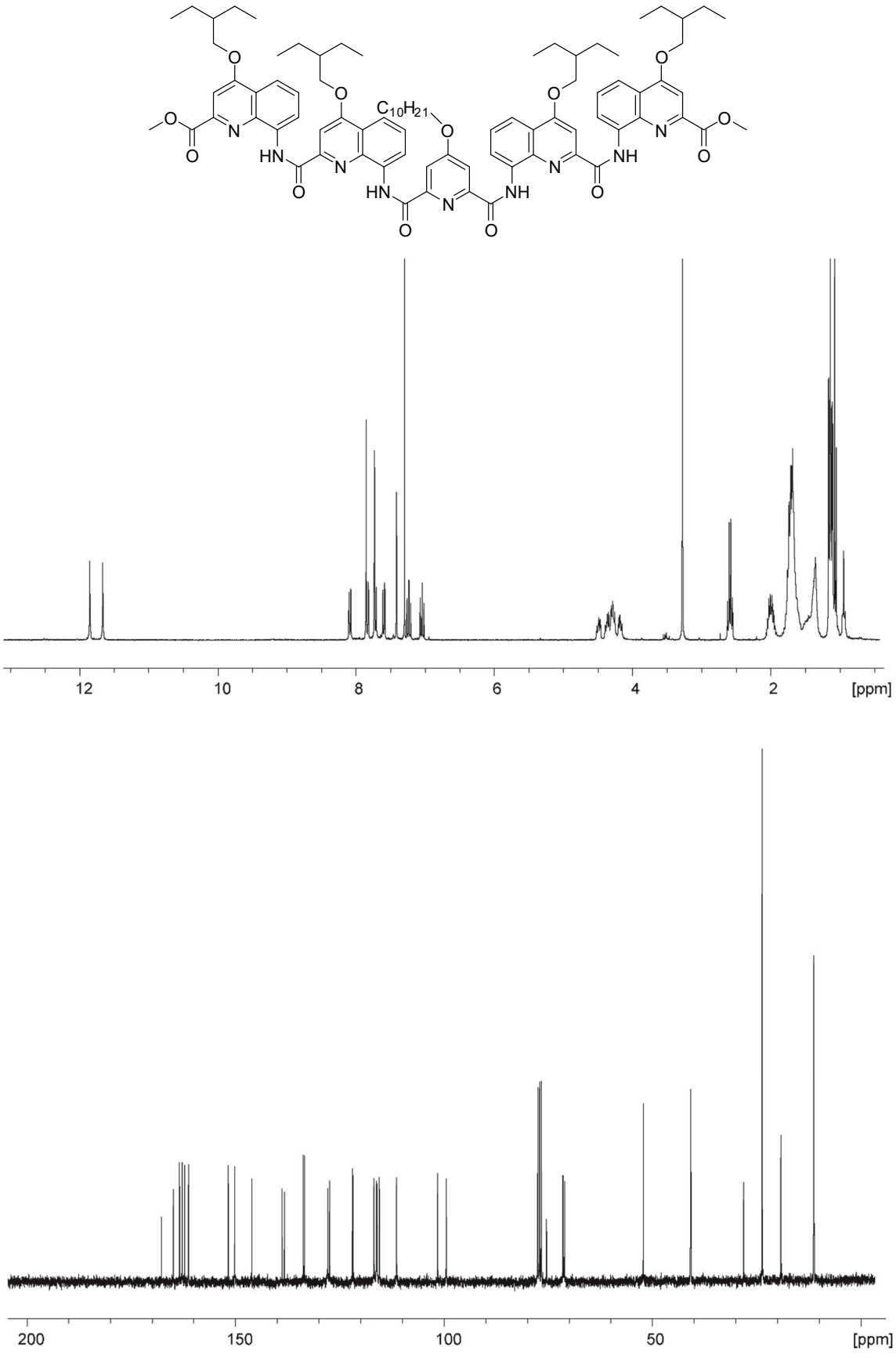

Figure S43. ^{1}H and ^{13}C NMR spectra of a $CDCl_3$ solution of **Me-Q_2PQ_2-Me**

H-Q_2PQ_2-H

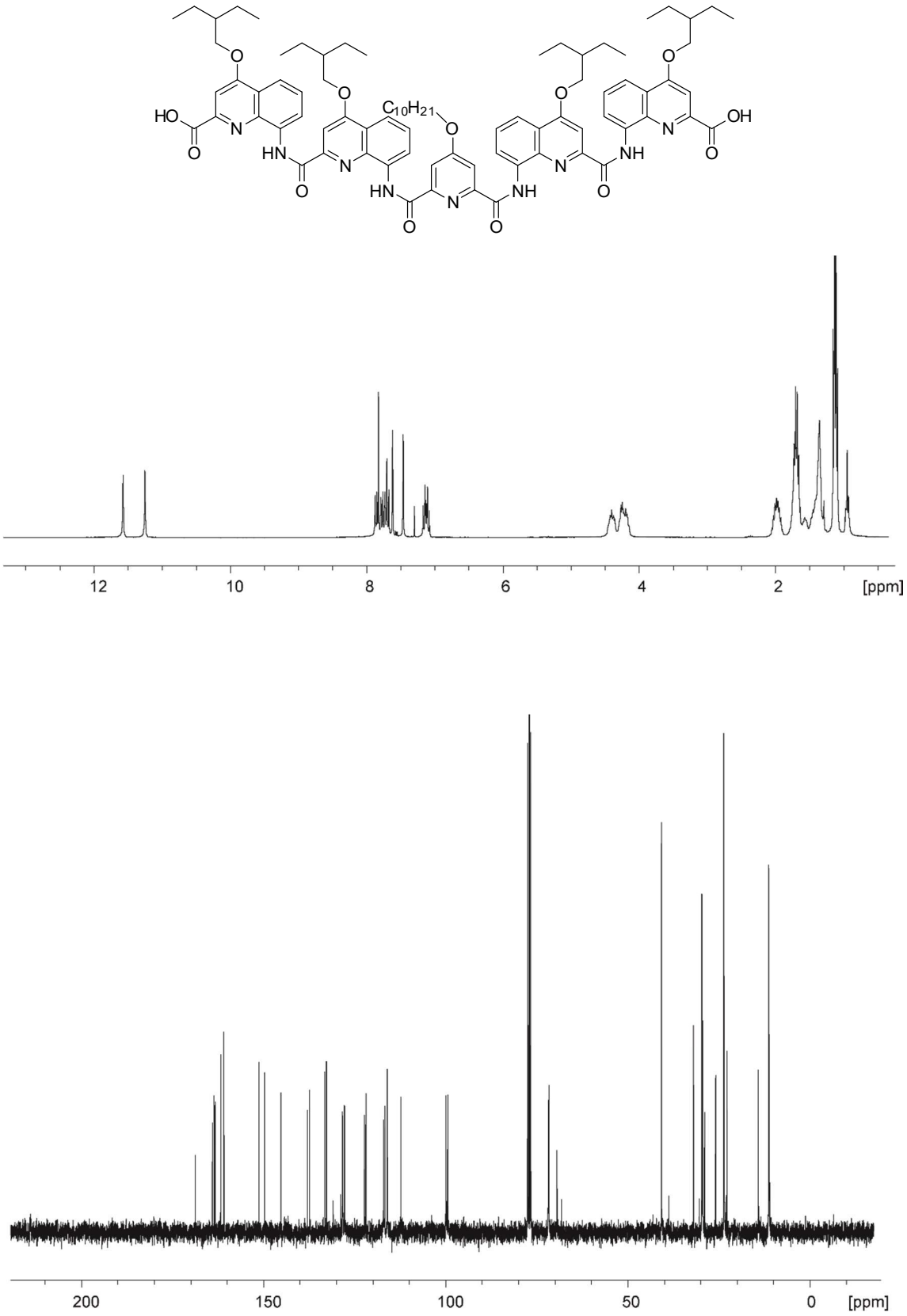

Figure S44. ^{1}H and ^{13}C NMR spectra of a $CDCl_3$ solution of **H-Q_2PQ_2-H**

[i] J. Wang, H. Little, J. Duhamel, X. Li, M. Nagula, V. Maurizot, I. Huc, "Dimensions of Quinoline-Based Foldamers Labeled with Oligo(phenylene vinylene) Probed in Solution by Time-Resolved Fluorescence Anisotropy" *Macromolecules* **2019**, *52*, 5829-5837.

[ii] H. Little, J. Wang, J. Duhamel, X. Li, M. Nagula, V. Maurizot, I. Huc, "Simplification in the Acquisition and Analysis of Fluorescence Decays Acquired with Polarized Emission for Time-Resolved Fluorescence Anisotropy Measurements" *Anal. Chem.* **2020**, *92*, 668-673.

[iii] T. J. Chuang, K. B. Eisenthal, "Theory of Fluorescence Depolarization by Anisotropic Rotational Diffusion" *J. Chem. Phys.* **1972**, *57*, 5094−5097.

[iv] T. Qi, T. Deschrijver, I. Huc, Large-scale and chromatography-free synthesis of an octameric quinoline-based aromatic amide helical foldamer, *Nature Protocols* **2013**, *8*, 693-708.

[v] X. Li, T. Qi, K. Srinivas, S. Massip, V. Maurizot, I. Huc, Synthesis and multibromination of nanosized helical aromatic amide foldamers via segment-doubling condensation, *Org.Lett*. **2016**, *18*, 1044-1047.

[vi] V . Berl, I. Huc, R. Khoury, J.-M. Lehn "Helical molecular programming. Folding of oligopyridine-dicarboxamides into molecular single hélices" *Chem. Eur. J.* **2001**, *7*, 2798-2809